In-situ Adsorption of Gold(III) Chloride on Activated Carbon Under Pressure Oxidation-Leaching Conditions

Jean-Christophe Parisien-La Salle

Department of Mining and Materials Engineering
McGill University, Montreal, Canada
May 2012

A thesis submitted to McGill University
in partial fulfillment of the requirements of the degree of
Master of Science

ABSTRACT

The focus of this research is the interaction of gold(III)chloride with activated carbon in acidic sulphate solutions. More specifically in this research the in-situ adsorption of gold (III) chloride on activated carbon within an autoclave in the presence of iron sulphide oxidation products, is investigated. Two types of experiments are presented in this research. In the first one, gold(III) chloride (1.5×10^{-4} M Au(III) plus 0.05 M extra chloride) was allowed to adsorb onto activated carbon (10, 20 and 30 g/L) at pH 1.5 and at different temperatures (22, 60 and 95 ^{o}C). Complete gold removal was achieved within a few minutes of contact. The kinetics were found to increase with increasing carbon loading as well as temperature and exhibit "first order" diffusion-controlled behaviour. However an increase in chloride concentration from 0.05 M to 1 M was found to slow down gold adsorption. Via X-ray photoelectron spectroscopic analysis (XPS), it was determined that gold undergoes a reduction upon adsorption on carbon and is present partly as Au(I)Cl and partly as metallic gold. The relative amount of metallic gold increased with temperature but decreased with high chloride ion concentration.

The second type (carbon-in-autoclave) of experiment involved pressure leaching (at 155 and 200 ^{o}C) of pyrite particulates (acting as model sulphide mineral) spiked with metallic gold (precipitated via cementation) in the presence of low chloride ion concentration and activated carbon. Under these conditions gold was found to lixiviate forming gold chlorocomplexes that reported (in part) on the available activated carbon. The loaded gold, analyzed by XPS was found to be ~2/3 metallic and ~1/3 Au(I)Cl. Because of a "preg-robbing" effect exhibited by hematite forming in-situ, excess sodium was added to the system favouring natrojarosite as the latter has no affinity for gold. In this way gold loading on carbon was maximized. However, significant occurrence of gold deposition on metallic surfaces was observed. By using a glass autoclave the gold plating occurrence was eliminated allowing up to 97% recovery of gold on the activated carbon. Similar results were obtained when copper concentrate material was substituted for pyrite. This work shows that even in small chloride ion concentrations (<0.2 M) gold is easily leached under autoclave oxidation conditions allowing conceptually for its in-situ recovery on activated carbon.

RÉSUMÉ

L'objectif de cette recherche est d'analyser le comportement du complexe Au(III)Cl4- en contact avec du charbon actif dans un environnement hydrométallurgique acide contenant des ions de sulfate. Cette recherche détaillera plus précisément l'adsorption du complexe Au(III)Cl_4^- sur le charbon actif dans un autoclave à température et pression partielle d'oxygène élevée en présence des produits d'oxydation de sulfure de fer. Cette recherche présentera deux types d'expériences. En premier lieu, le chlorure d'or(III) ($1.5x10^{-4}$ M Au(III) et 0.05 M chlorure) a été adsorbé sur le charbon actif (10, 20, 30 g/L) à un pH de 1.5 et à différentes températures (20, 60 et 95 ^oC). Le complexe aurifère est complètement adsorbé par le charbon actif après quelques minutes. La cinétique augmente proportionnellement avec une augmentation de la teneur d'or sur le charbon actif de même qu'avec l'augmentation de la température tout en présentant un comportement de diffusion du premier ordre. Toutefois, une augmentation de la concentration de chlorure de 0.05 M à 1 M ralentit l'adsorption d'or sur le charbon actif. Suite à une analyse par rayons-X spectroscopiques photoélectriques (XPS), il a été possible de déterminer que le complexe aurifère (Au(III)Cl_4^-) subit une réduction sur le charbon actif et est présent en partie comme or natif (métallique) et or complexé Au(I)Cl. La quantité relative d'or métallique adsorbée sur le charbon actif augmente avec la température, mais diminue avec une concentration de chlorure élevée.

Le deuxième type (Carbon-in-autoclave) d'expérience consiste à oxyder sous pression (à 155 ^oC et 200 ^oC) des particules de pyrite (agissant comme minerais de sulfure idéal) dopé avec de l'or métallique (précipité via cémentation) en présence d'une faible concentration d'ions de chlorure et de charbon actif. Dans cet environnement, l'or est lixivié formant des chlorocomplexes d'or qui ont été adsorbés (en partie) sur le charbon actif. L'or chargé sur le charbon actif a été analysé par XPS et les résultats démontrent la presence de 2/3 métallique et 1/3 Au(I)Cl. Suite au phénomène de « preg-robbing » dû a l'hématite formée durant l`oxydation de la pyrite, un surplus de sodium a été ajouté afin de favoriser la formation du natrojarosite qui n'a aucune affinité avec le chlorure d'or(III). Ainsi, l'adsorption de l'or sur le charbon actif est maximisée. Toutefois, une cémentation importante d'or a été observée sur les surfaces métalliques internes de l'autoclave. En utilisant un autoclave en verre, la quantité d'or plaqué a été éliminé permettant ainsi une récupération de 97% d'or sur le charbon actif. Des résultats similaires ont été obtenus lorsqu'un concentré aurifère de cuivre a été oxydé à la place de la pyrite. Ce travail démontre donc que même de faibles concentrations de chlorure (<0.2M) peuvent facilement lixivié l'or métallique en autoclave permettant théoriquement sa récupération sur du charbon actif durant le procédé d'oxydation.

ACKNOWLEDGEMENTS

I would like to thank Professor Demopoulos for giving me this opportunity to work with him, and allowing me to work in an area of research, which is very important to me. I would also like to thank him for his guidance and especially patience, which has resulted in a unique learning experience.

I would like to thank Levente Becze for his unparalleled guidance, Mario Gomez for his help with the XPS analysis, as well as Cecile Charbonneau for her help with the SEM characterization. I would like to thank specially Derek Blais and Renaud Daenzer for their insight and help throughout this project. Lastly I would like to acknowledge the remaining members of the hydrometallurgy group, as well as Monique Riendeau, Barbara Hanley, Terry Zatylny and Matthew Lagace for their help throughout these last two years.

I would also like to thank my family and friends for supporting me throughout this endeavour.

TABLE OF CONTENTS

LIST OF FIGURES

LIST OF TABLES

Chapter 1. **INTRODUCTION**

Gold ores may be classified broadly as “free-milling” and “refractory” ores. By the term “refractory” gold ores, reference is made in general to ores in which gold is partly or completely encapsulated / locked within a mineral that is difficult to leach like arsenopyrite or pyrite. As such, an oxidative pre-treatment is necessary to liberate the gold, essentially equivalent to “chemical digestion” before cyanidation is applied. Among the various oxidative pre-treatment technologies pressure oxidation (POX) is by far the most widely used. This hydrometallurgical process generates an acidic slurry/residue consisting mostly of precipitated in–situ iron (hydroxy) oxides and sulphates from which following thorough washing (CCD) and neutralization gold is recovered by alkaline cyanidation. Another process where gold is recovered from the residue generated in an autoclave is copper pressure leaching. There are two general approaches in pressure leaching of copper: the high-temperature, or total sulphur oxidation and the medium-temperature approach, exemplified by the CESL process. Drawbacks of this technology are: in the former case excessive cost due to oxygen consumption and neutralization of the generated acid; and in the latter case low gold recoveries due to the formation of elemental sulphur which interferes with cyanidation. Cyanidation remains by far the key process used world-wide, on “free-milling” ores and on gold recovery systems from autoclave discharge. Increasingly serious concerns are expressed about the toxicity of cyanide and the risks associated with its handling and transportation.

It is the scope of this thesis to investigate a new cyanide-free and direct (one-step) concept for the recovery of gold from refractory gold pressure oxidation and copper pressure leaching reactors-autoclaves. The new process involves the extraction of gold during the actual pressure oxidation/leaching operation in the autoclave via the use of a small amount of chloride ion addition (if not already present) plus activated carbon. For maximizing gold recovery the process is designed in such way that favours the precipitation of iron as sodium jarosite since the latter does not interfere with gold recovery in contrast to hematite that does [1]. Under these conditions gold (in the form initially of aurochloride complex) adsorbs on carbon from which it can be recovered following screening, elution and electrowinning or reductive precipitation/cementation. The innovative aspect of this work is the use of activated carbon directly in the autoclave (“carbon-in autoclave”-CIA) which allows in the presence of small amount of chloride ions and the simultaneous precipitation of iron as jarosite to capture-recover gold in-situ hence potentially eliminating the downstream operations of CCD, neutralization and especially cyanidation. The following chapters, include a review of the relevant technical literature (Chapter 2) and a description of the experimental procedures used (Chapter 3); the obtained results are described the following way. Chapter 4 deals with the adsorption of gold(III) chloride on activated carbon in acidic mixed sulphate-chloride media under atmospheric pressure over the temperature range 20-95 ^{o}C as well as the XPS characterization of the corresponding gold loaded activated carbon. Chapter 5 describes the carbon-in-autoclave experiments over the temperature range 155-200 ^{o}C and the integration of the carbon-in-autoclave concept in terms of refractory gold ore treatment and copper pressure leaching operations. Lastly Chapter 6 summarizes the major conclusions from this study.

Chapter 2. LITERATURE REVIEW AND THEORY

2.1 GOLD RECOVERY-BRIEF HISTORICAL OVERVIEW

Gold has been one of the most sought after metals throughout history. It is one of the metals, which requires very little transformation from its native elemental state. It is recovered, historically by amalgamation [2,3] before it can be processed into various monetary and decorative objects. Initially gold was recovered from alluvial deposits. However these deposits have been essentially exhausted due to their ease of separation (by gravity methods) over the early years of gold rushes and later on industrial mining. Thus progressively more complex gold ores (gold associated with sulphide minerals) were discovered, the processing of which with the traditional recovery methods was inefficient yielding poor recoveries. This prompted the advent of new recovery technologies. The first industrially employed hydrometallurgical recovery method involved bubbling chlorine gas into a pulp to simultaneously oxidize and dissolve gold, which was subsequently precipitated out of solution by a reducing agent [2,3]. This recovery method was costly and had varying recoveries depending on the elements present in the ore. Therefore it has fallen out of practice until a recent renewal in interest. In 1887 a new process was developed in the United States, which used air (oxygen) and cyanide to oxidize and dissolve gold, in an alkaline medium. The solubilised aurocyanide complex was recovered by cementation out of solution using zinc as a reducing agent (Merrill Crowe Process). The cyanide-based gold recovery process was suitable for low grade ores and yielded 95% recoveries on sulphide ores. The addition of activated carbon to the pulp to promote adsorption of the complexed gold was introduced as early as 1949 [3]. However the activated carbon was smelted to recover gold. Beginning in 1952 gold stripping by employing the Zadra process was used to recover gold industrially [3]. Cyanidation of free-milling ores, as of 2006 accounted for 55 % of gold production worldwide [4].

2.2 REFRACTORY GOLD RECOVERY

Gold ores may be classified broadly as “free-milling” and “refractory” ores. Free-milling means that the ore, following some degree of preparation like crushing/grinding or flotation, is subjected to leaching in aerated alkaline cyanide media. Upon solubilization in the cyanide leach medium gold is recovered either via the Merrill Crowe zinc dust cementation process (following solid/liquid separation) or the most common CIP process (Carbon-in-Pulp). In the latter case, gold is eluted from the carbon and recovered from the eluate by electrowinning as *dore* metal [2]. Cyanidation remains by far the key process used worldwide, but increasingly serious concerns are expressed about the toxicity of cyanide and the risks associated with its handling and transportation [5,6,7]. As a result of these concerns there has been a lot of interest in investigating other lixiviant reagents than cyanide including halogen ions (chloride, iodide, and bromide), various thiosulphates, ammonia and sulphide ions [8,9].

The term “refractory” gold ores refers in general to ores in which gold is partly or completely completely encapsulated/locked within a sulphide mineral that is difficult to leach like arsenopyrite or pyrite. As such these ores are not amenable to direct cyanidation. Instead they require an oxidative pre-treatment via which the sulphide and arsenide minerals are decomposed and the trapped sub-microscopic gold is liberated. Following this oxidative pre-treatment the oxidized material is subjected to cyanidation as done with the free-milling ore. For the oxidative pre-treatment of refractory gold ores a variety of processes have been developed [2,4,10,11], The first commercially employed method consisted of roasting the ore or concentrate in an oxidizing atmosphere and obtaining a porous calcine from which gold was recovered by cyanidation. This method of roasting the ore and oxidizing the sulphides into sulphur dioxide gas and the arsenides into arsenic trioxide gas has fallen out of favour lately due to economic and environmental concerns. Over the past 25 years as alternatives to roasting, a new technology called pressure oxidation (POX) and to a lesser extent another technology called bio-oxidation/leaching (BIOX) have been introduced to refractory gold pretreatment practices. By far POX dominates today the industrial practice of gold recovery from refractory ores [2]. The relevant chemistry and kinetics of the two most important refractory gold mineral carriers, namely pyrite and arsenopyrite has been described in literature by *Papangelakis and Demopoulos* [11,12,13,14]. Typically in this process temperatures above 190°C (up to 250°C) are employed and oxidation occurs in an acidic sulphate environment. One of the objectives of pressure oxidation is the complete oxidation of all sulphide sulphur to sulphate, as formation of elemental sulphur, which is favoured at lower temperatures is detrimental to subsequent gold recovery by cyanidation. Most of iron and arsenic precipitates during POX processing in-situ, i.e. inside the autoclave, in the form of hematite [15], jarosite [16] and iron arsenate compounds [17]. It is from these precipitated/oxidized solids that gold is recovered following solid/liquid separation, washing, and neutralization by cyanidation.

Another process where gold is recovered from the residue generated in an autoclave is copper pressure leaching. Copper pressure leaching involves oxidation of flotation concentrates made of copper minerals like chalcopyrite or even enargite. During pressure leaching copper reports into the solution while the bulk of iron (and any arsenic if present) precipitates in situ typically as hematite or jarosite [18] and if arsenic is present as scorodite [19]. There are two general approaches in pressure leaching of copper: the high-temperature, or total sulphur oxidation, approach exemplified by the Phelps-Dodge (now Freeport-McMoRan) operation in Bagdad, Arizona [20], and the medium-temperature approach, exemplified by the CESL process [18,21,22]. In the first option sulphide sulphur is oxidized completely to sulphate sulphur to avoid the complications of elemental sulphur during downstream cyanidation. In this way this process option resembles POX. The drawback of this process is its high cost due to excessive oxygen consumption and acid generation that requires neutralization. On the other hand the medium-temperature option is challenged when it comes to gold recovery from its residue because of the presence of elemental sulphur that interferes with cyanidation. This has prompted companies to investigate on a variety of alternatives that either have proven not feasible for large scale operations or ineffective or simply costly. More recently pressure cyanidation that employs short retention time has been adopted by Teck for their CESL Process [22,23]. This issue, i.e. economic and clean gold recovery from the copper pressure leach residue, has in many instances hampered or completely stopped the industrial implementation of several of the pressure leaching operations.

2.3 NATURE OF REFRACTORY GOLD

In general, ores are deemed "refractory" when gold recoveries by cyanidation alone are below 80 %. The root-cause in ores, which are deemed refractory, can be attributed to two factors [7,10, 24-26], i.e. essentially there are two types of refractory gold ores:

- Type I-Occlusion or dissemination of gold as small grains or as solid solution within an iron sulphide/arsenide matrix, or other mineral. Depending on the ore body, gold can be part of the crystal lattice, most notably in arsenopyrite, the most common gold bearing refractory iron sulphide [24,27].
- Type II-Other minerals which do not lock up the gold yet interfere with its recovery by uptaking via physical or chemical adsorption of complexed gold species [28]. Among these interfering substances/minerals are: carbonaceous matter, amorphous or graphitic carbon, humic acid and certain clays [10]. The refractory properties of gold ores containing carbonaceous matter cause the so-called "preg-robbing" effect according to which these ores adsorb gold liberated from the matrix and thus result in poor recovery.

2.4 PRESSURE OXIDATION

2.4.1 Pyrite and arsenopyrite oxidation

Oxidation pre-treatment processes account for 10% of global gold production, of this, whole ores and concentrate pressure oxidation account for half [4]. Ores which undergo pressure oxidation are mainly the first type of refractory gold ores in which gold is locked inside iron sulphides/arsenides. The oxidation chemistry and kinetics of pyrite and arsenopyrite is reported elsewhere [11-14, 29-39]. By focusing on pyrite oxidation it can be stated that depending on the temperature and oxidizing environment two competing reactions may take place leading to either elemental sulphur or sulphate sulphur formation (see reactions (1) and (2) [29, 40]. At high temperatures (>180 °C), however, reaction (1) dominates.

$$FeS_2 + H_2O + \frac{7}{2}O_2 \rightarrow FeSO_4 + H_2SO_4 \quad (1)$$

$$FeS_2 + 2O_2 \rightarrow FeSO_4 + S^o \quad (2)$$

Upon the formation of ferrous ions, they are oxidized further to ferric ions (reaction (3)), which undergo hydrolysis in-situ yielding different precipitation products depending on the prevailing solution conditions such as hematite, jarosite, basic ferric sulphates, etc.

$$FeSO_4 + H_2SO_4 + \frac{1}{2}O_2 \rightarrow Fe_2(SO_4)_3 + H_2 \quad (3)$$

Mechanistically the oxidation of pyrite can be viewed as an electrochemical reaction. Thus Bailey and Peters [29] established the respective anodic and cathodic half-reactions and showed that water is the oxygen source for the oxidation of sulphide sulphur into sulphate (reaction 4 with the cathodic reduction of dissolved oxygen happening on different sites of the pyrite surface (reaction 5).

$$Anodic: {FeS_2}^{(-1)} + 8H_2O \rightarrow Fe^{2+} + 2S^{(+6)}O_4 + 16H^+ + 14e^- \quad (4)$$

$$Cathodic: \frac{1}{2}O_2^{(0)} + 2H^+ + 2e^- \rightarrow H_2O^{(-2)} \quad (5)$$

In addition to oxygen reduction on pyrite surface (Equation 5) it has been established as well that the oxidation of pyrite proceeds via the involvement of the ferric/ferrous couple [33]. The direct oxidation of pyrite by ferric ions is described by reaction (6).

$$FeS_2 + 14Fe^{3+} + 8H_2O \rightarrow 15Fe^{2+} + 2SO_4^{2-} + 16H^+ \quad (6)$$

The dual involvement of ferric and oxygen in the oxidation of pyrite and other iron sulphides in general has been further verified by many researchers [30, 34-38].

2.4.2 In-situ iron precipitation

As already mentioned during pressure oxidation the solubilised iron undergoes hydrolysis and precipitates. Depending on temperature, oxygen pressure and solution composition parameters such as acidity, total sulphate content and presence of co-ions for example sodium, many products can precipitate, the most common of which being hematite. This can be evaluated from the 200 ^{o}C Fe-S-H_2O Pourbaix diagram shown in Figure 1 according to which hematite is the thermodynamically stable phase over a wide pH (>0) and oxidizing potential (E_h>~0.3V at pH~1) range [30-32]. At lower potentials, pyrite remains stable; therefore it is primordial for applying a highly oxidizing environment to obtain complete oxidation. Finally the diagram clearly shows that the predominant oxidized sulphur species is sulphate/bisulphate under POX (low pH and high E_h) conditions.

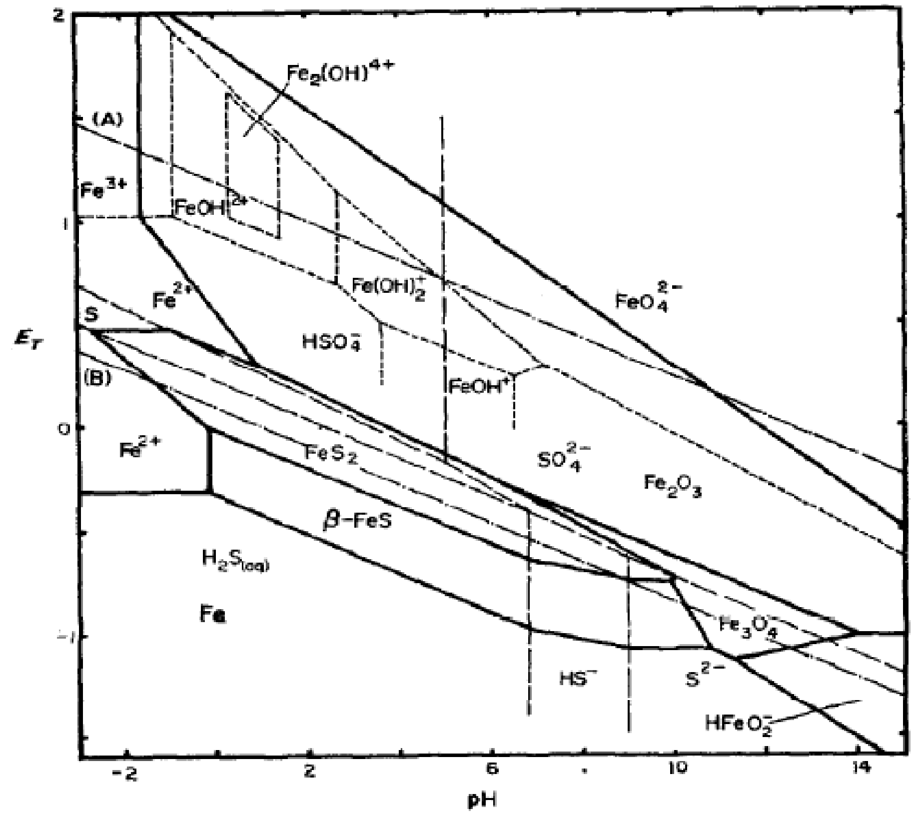

Figure 1: Eh vs. pH diagram for the Fe-S-H_2O system at 200 ^{o}C (a_{Fe}=1, a_S=1) [41].

However, the picture presented in Figure 1 refers to thermodynamically stable phases forming from pure Fe-S-H_2O solutions. Kinetic factors combined with the presence of several cations such as lead, sodium and silver, released from the leaching of the sulphide feedstock, may lead instead to formation of other iron precipitates like basic ferric sulphate and jarosite; the latter's general formula being $MFe_3(SO_4)_2(OH)_6 \cdot xH_2O$,, where M may be H_3O^+, K^+, Na^+, NH_4^+, Ag^+ or $1/2Pb^{2+}$ [33-35]. The precipitation of natrojarosite is represented by equation (7).

$$3Fe_2(SO_4)_3 + Na_2SO_4 + 12H_2O \rightarrow 2NaFe_3(SO_4)_2(OH)_6 + 6H_2SO_4 \tag{7}$$

Several factors have been established in promoting jarosite precipitation such as temperature range (refer to Figure 2 [16], ferric concentration, acid concentration, alkali metal ion concentration and the presence of seed [16]. Jarosite precipitation may also occur from mixed sulphate/chloride media as long as jarosite-forming cations like sodium or silver are present [42]. The kinetics for the atmospheric formation of jarosite (at ≤98 ^{o}C) are very slow [43, 44]. However in the presence of seed crystals the induction period for the precipitation is eliminated and the precipitation rate increases linearly with increase in seed concentration. No investigation into the effect of seed crystals on jarosite precipitation in autoclaves as the system studied here has been reported.

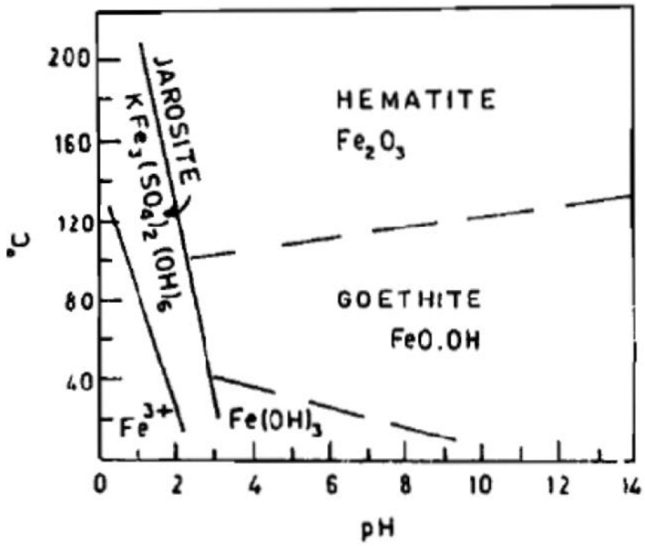

Figure 2: Stability region of natrojarosite relative to pH and temperature [16]

2.5 GOLD BEHAVIOUR DURING PRESSURE OXIDATION

During pressure oxidation, generally no or very little complexing ligands (like halide ions) are present, hence the common understanding is that gold remains in the elemental state if already present as such or simply converts to that as soon as it is liberated. It is conceivable that temporarily solubilised gold is reduced in-situ on oxidized mineral product surfaces via short-term adsorption or not and reports with the residue solids. Gold is subsequently recovered from these residues by cyanidation under an oxidizing environment. However in the presence of significant amounts of complexing agents like chlorides, arising from either brackish process water or the ore itself can lead to greater gold solubilization and possible losses.

A classic example of solubilising gold, which caused serious complications was at the Lihir POX plant in Papua, New Guinea. In this case chlorides caused the solubilisation of gold within the autoclave and the subsequent plating of gold inside the discharge nozzle [45]. More recently gold losses due to solubilization of gold as a result of chloride complexation was reported by Agnico-Eagle [46].

Gold has two oxidation states: aurous (Au^{1+}) and auric (Au^{3+}). These are stabilized only upon complexation with strong ligands. Thus the solubilisation of gold in cyanide solutions occurs via the formation of the cyano-aurous complex $Au(CN)_2^-$, while in the presence of halide ions gold is solubilised in its auric form [47,48] as $Au(Cl)_4^-$.

The importance of complexation in rendering gold soluble can be evaluated by referring to appropriate reduction potentials and Pourbaix diagrams. Equation 8 gives the standard reduction potential corresponding the Au^{3+}/Au couple. When this potential is compared to that of oxygen/water couple (Equation 9) it becomes clear that gold in its elemental state is the most stable form.

$$Au^{3+} + 3e^- \rightarrow Au_{(s)}\ e^o = 1.498V \quad (8)$$

$$\tfrac{1}{2}O_2 + 2H^+ + 2e^- \rightarrow H_2O\ e^o = 1.23V \quad (9)$$

With the presence of chloride ions as a complexing agent, the potential required for the oxidation of gold does change and allows for the lixiviation of the metal since its standard reduction potential now (0.99V) is less than that of oxygen (1.23V).

$$AuCl_4^- + 3e^- \rightarrow 4Cl^- + Au_{(s)}\ \ e^o = 0.99V \quad (10)$$

This can be further exemplified with the help of the Au-H_2O (Figure 3) and Au-Cl-H_2O (Figure 4) Pourbaix diagrams [49].

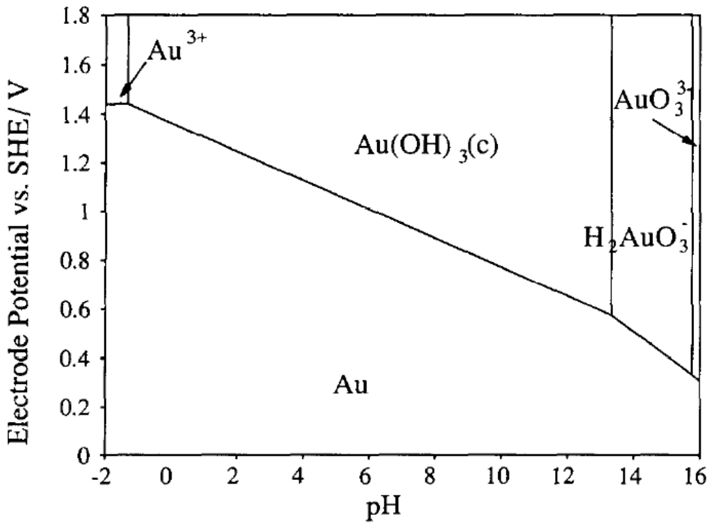

Figure 3: Pourbaix diagram of the Au-H_2O system at 25 ºC. (a_{Au}=10^{-3}) [49]

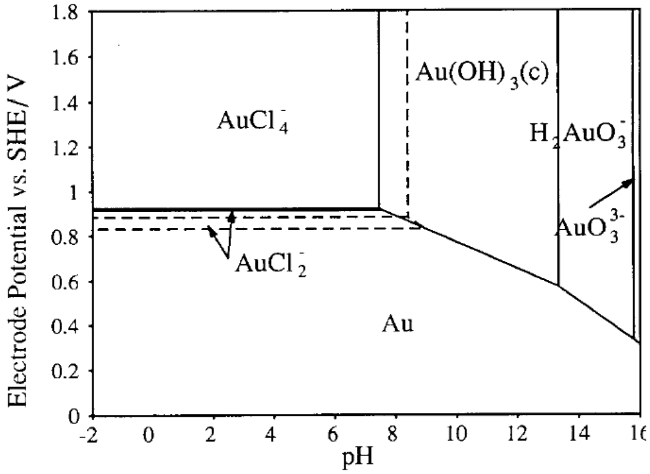

Figure 4: Pourbaix diagram of the Au- Cl-H_2O-system at 25 ^{o}C. (a_{Au}= 10^{-3}, a_{Cl} = 1)[49]

It is interesting to report here that with increasing temperature the reduction potential of the $Au(Cl)_4^-$/Au couple decreases making the oxidation of gold possible even by the Fe^{3+}/Fe^{2+} couple as it can be deduced from the data plotted in Figure 5 [48].

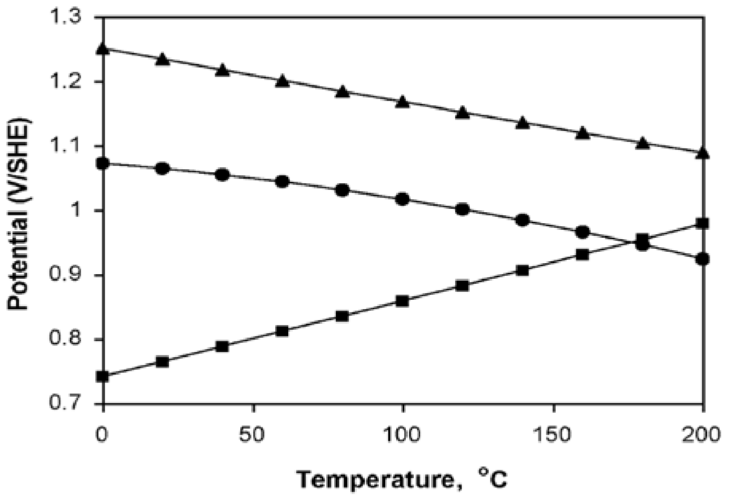

Calculated equilibrium potentials for the Fe^{3+}/Fe^{2+}(■), the $AuCl_4^-$/Au (●) and the O_2/H_2O (▲) couples. $[AuCl_4^-] = 10^{-5}$ M, $[Cl^-]=0.01$M, $[H^+] = 1$ M

Figure 5: Reduction potentials of the $AuCl_4^-$/Au, O_2/H_2O and Fe^{3+}/Fe^{2+}couples as a function of temperature. ($[Fe^{3+}]=[Fe^{2+}]=0.1$M) [48]

The possible dissolution of gold during pressure oxidation as a result of the presence of chlorides and the relative stability of gold(III)-chlorocomplexes as a function of temperature and chloride ion concentration was studied recently in our laboratory by Blais using the OLI thermodynamic software package (StreamAnalyzer Version 3.0) [1]. A sample of his calculations is presented in Figure 6; the calculations were made for $5x10^{-4}$ M of $AuCl_3$ (corresponding to approximately 100 mg/L Au). Therefore, according to this data the concentration of stable soluble gold complex decreases upon a temperature rise, but increases upon raising the excess chloride ion concentration. For example Blais calculated that the solubility limit of the gold (III) chloride complex before it is reduced to metallic gold for the case of a 0.0715M HCl (or 2.3g/L Cl) solution is

$5x10^{-4}$ (or 100mg/L) Au at 227 °C.

Although in industrial systems this may be much lower nevertheless these numbers serve to substantiate the notion that solubilization (even if partial or temporary, i.e. metastable) of gold can occur hence the importance of considering its possible in-situ recovery.

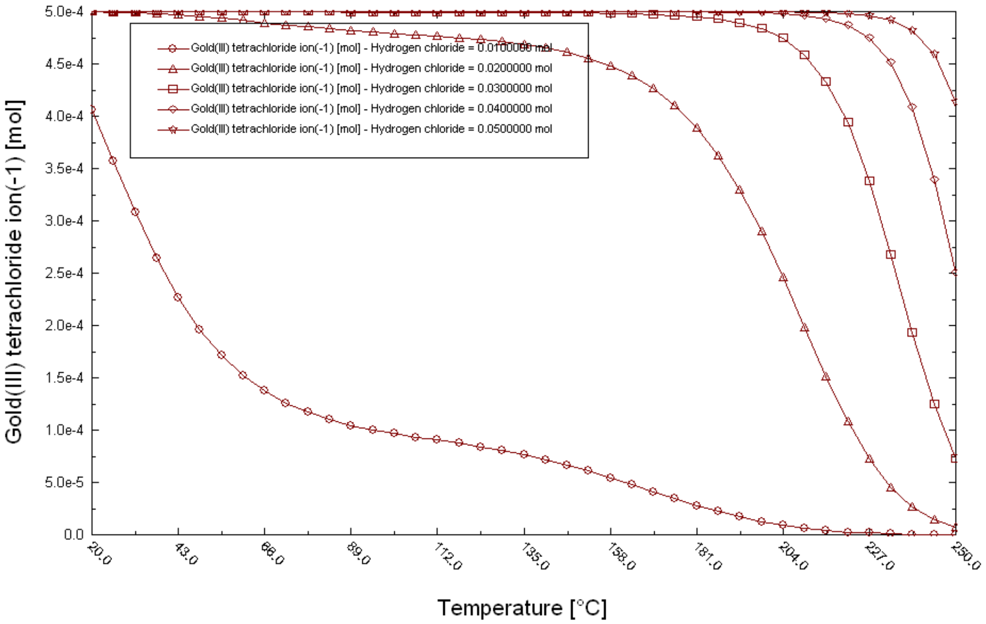

Figure 6: The effect of temperature on gold (III) chloride complex concentration for various added amounts of excess chloride (as HCl) [1]

2.6 ADSORPTION OF GOLD (III) CHLOROCOMPLEXES

2.6.1 General aspects of adsorption

Adsorption of a chemical species on a surface may be of two types, chemical adsorption and physical adsorption. In physisorption the interaction is dominated by Van Der Waals forces between the adsorbate and the substrate. This type of physical interaction is weak in nature and exothermic in the range of 20 kJ/mol [50]. In the case of gold cyanide complex adsorption onto activated carbon, this occurs via physisorption [51,52], and this is why its elution by the Zadra process takes place at high temperatures (>90 ^{o}C).

Chemisorption on the other hand involves chemically bonding of the adsorbate onto the substrate via covalent bonds. This type of adsorption is much stronger and due to the high activation energy required to forge covalent bonds is slower than physisorption. This type of adsorption exhibits in general endothermic character at low temperatures and exothermic nature at very high temperatures [53]

2.6.2 Adsorption of gold(III) chloride on iron precipitates

Complexes of gold including gold(III) chloride are known to adsorb on iron (hydroxy)oxides via chemisorption. Thus according to Karasyova et al. gold(III) chloride adsorbs on hematite via inner sphere coordination [54,55]. But in addition to complexes, colloidal gold has been reported to adsorb on iron oxide particles due to electrostatic attraction. This phenomenon is known as mutual coagulation or heterocoagulation [56]. This type of electrostatic interaction may lead to re-encapsulation hence constituting a possible cause of gold losses during pressure oxidation processes. This solubilisation-encapsulation phenomenon apparently is observed in natural mineralization processes theorized to be responsible in the genesis of refractory gold ores (gold encapsulated within iron sulphides upon cooling) [57]. In this case the adsorption mechanism of gold(III) chloride on the surface of iron sulphides (see pyrite) is of electrostatic (physisorption) type followed by reduction on the mineral surface as represented by equation 11 [58,59].

$$FeS_2 + 5AuCl_4^- + 8H_2O \rightarrow Fe^{3+} + 2SO_4^{2-} + 16H^+ + 5Au_{(s)} + 20Cl^- \qquad (11)$$

By extrapolating this geochemical information to the case of pressure oxidation of refractory gold ores, it may be deduced that partially oxidized sulphides (e.g. pyrite or arsenopyrite) plus in-situ forming hematite or other oxidized products can cause equivalent to “preg-robbing” effect if chloride ions are present.

The possible “preg-robbing” effect of precipitated iron phases on gold(III) chloride complexes under pressure oxidation conditions was recently investigated by another member of McGill’s Hydrometallurgy Group [1]. Thus in this study hematite precipitation from sulphate solutions was carried out at 200 °C in the presence of 100 mg/L Au ($5x10^{-4}$ M $HAuCl_4$) plus 0.05 M HCl (Cl/Au molar ratio =100). As it can be seen in Figure 7 [1] all gold was found to coprecipitate with hematite. After characterization of the gold/hematite precipitate, Blais concluded that at least 50% of gold was present in the precipitate as adsorbed gold(III) chloride species and the rest in metallic state. The adsorption of gold(III) chloro-complexes onto the surface of hematite was suggested to be described by the following reaction (where $=FeOH$, symbolizes the surface of iron (hydroxyl)oxide:

$$=FeOH + AuCl_4^- \rightarrow = FeOHAuCl_3 + Cl^- \quad (12)$$

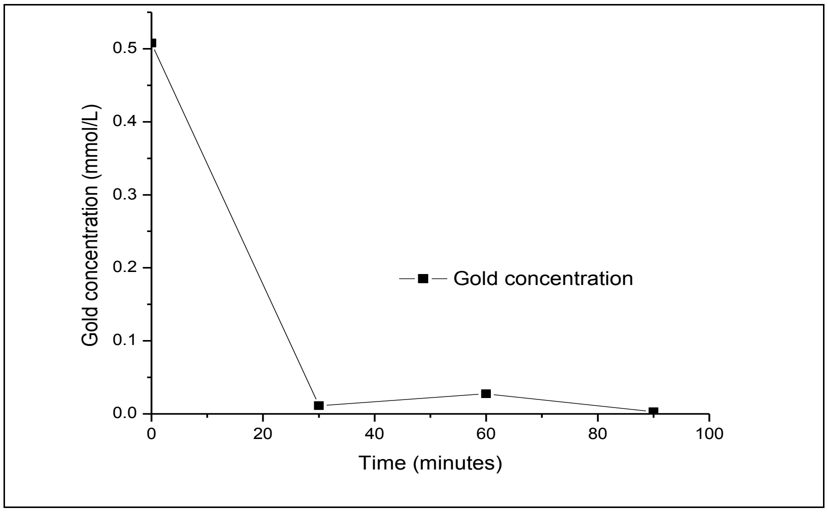

Figure 7: Gold concentration change with retention time during hydrolytic precipitation of hematite at 200 °C [1]

In contrast to hematite no gold was found to co-precipitate in other tests favouring the formation of natrojarosite, again at 200 °C. This is clearly seen with the data plotted in Figure 8 [1]. In other words in this case gold(III) chloride neither adsorbed nor was apparently chemically reduced. This finding was utilized in the present work focusing on the in-situ recovery of solubilised gold (in the presence of small amount of chloride ions) by activated carbon.

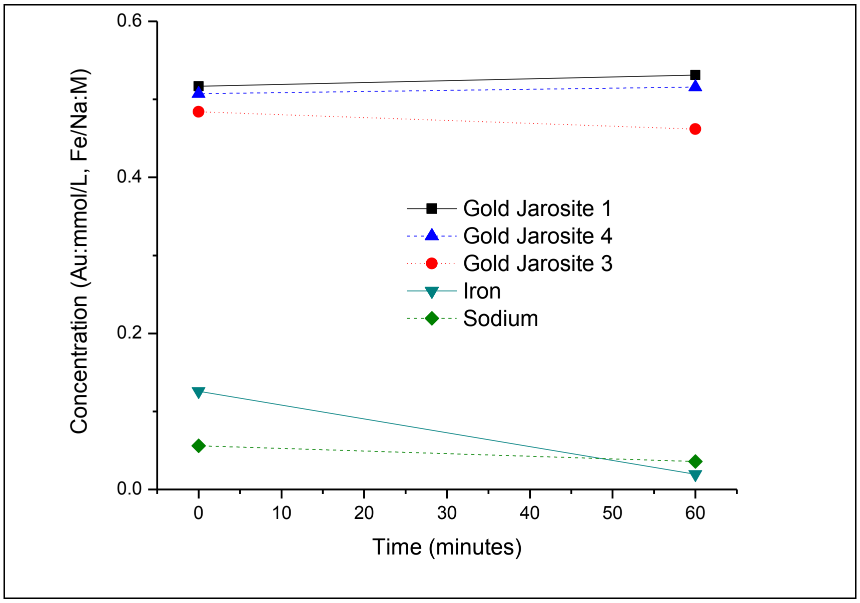

Figure 8: Gold, iron and sodium concentration profiles during triplicate natrojarosite precipitation tests in the presence of gold (III) chloride at 200 °C [1]

2.6.3 Adsorption of gold(III) chloride onto activated carbon

Conventionally in gold mining, the gold(I) cyanide complex $Au(CN)_2^-$ adsorbs onto activated carbon via Van Der Walls forces [52,60], i.e. via physisorption. This adsorption is reversible and at high temperature, the gold complex can be stripped off the activated carbon. However, in the case of gold(III) chloride adsorption onto activated carbon [61,62] chemical reduction occurs on the surface of the activated carbon resulting in metallic gold formation and apparent production of carbon dioxide as described by equation 13.

$$4AuCl_4^- + 3C + 6H_2O \rightarrow 4Au_{(on\ carbon)} + 12H^+ + 16Cl^- + 3CO_2\ E^o = 0.796V \qquad (13)$$

It has been further established that the adsorption/chemical reduction of gold chloride onto activated carbon is diffusion-controlled [61,62].

2.7 PROCESSING OF REFRACTORY GOLD ORES-THE POX PROCESS

The standard gold recovery flowsheet for a refractory ore involving pressure oxidation (POX) is shown in Figure 9. The feed, which has been crushed, milled and depending on the grade passed through a flotation bank for concentration, is sent to an autoclave in which is made to react in an acid solution (the acid, H_2SO_4, is generated in situ by the oxidation of sulphide minerals) with pressurized oxygen that is bubbled through the pulp continuously at temperature above 180 ^{o}C. The detailed analysis of the POX autoclave process has been described previously by Demopoulos and co-workers [63,64]. Once the host mineral sulphides are oxidized, gold is liberated and reports to the residue that forms in situ via the precipitation of iron (mostly) and other elements as oxides and sulphates. The product slurry from this pressure oxidation is sent to a counter-current decantation circuit where the solids (residue) are separated from the acidic solution and washed. The acidic discharge solution (barren in metal values) is sent to an acid neutralization stage. Calcium carbonate and/or calcium oxide (lime) are added to neutralize the acidic solution. Another solid/liquid stage further separates the underflow into tailings (mostly in the form of gypsum and iron hydroxides) and treated effluent (water), which can be recycled to the pressure oxidation stage. The underflow from the CCD circuit comprises the washed solids and the liberated gold. These solids are sent to another leaching stage where they are subjected to alkaline cyanidation (neutralized to pH 10-12 with lime and aerated in the presence of cyanide) in order to effect the dissolution of gold (as aurocyanide complex). Subsequently to cyanidation (or sometimes during cyanidation-this is called CIL-carbon-in-leach) the slurry is brought in contact with activated carbon (this is the so-called CIP, or carbon-in-pulp process). During CIL or CIP the gold-cyanide complex readily adsorbs onto the activated carbon. The gold-loaded carbon is separated by screening while the waste cyanide-laden solution/slurry is sent to a cyanide destruction plant. The gold-loaded carbon is forwarded to the elution section of the plant where the gold-cyanide complex is eluted from the activated carbon using a very concentrated and hot cyanide solution. Upon completion of elution, the eluate that contains the eluted gold-cyanide complexes is sent to electrowinning-EW (Au Recovery Box) where metallic gold (*dore* metal) is produced and carbon is recycled (after regeneration) back to the CIP operation.

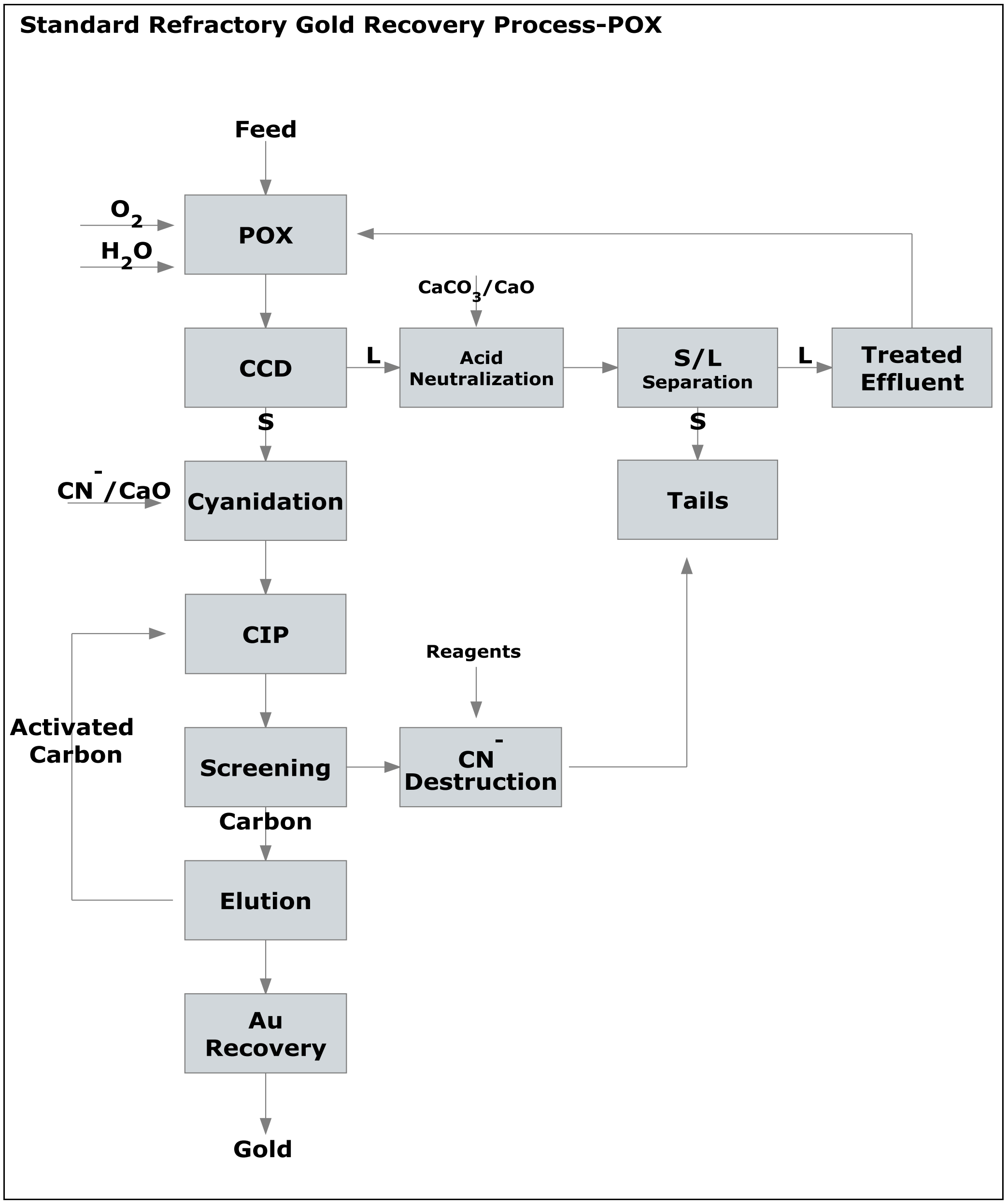

Figure 9: Schematic diagram of standard refractory gold recovery flowsheet by POX

In the standard POX process, which involves strictly sulphate solutions, the liberated gold reports as metallic grains in the residue from which it is recovered by cyanidation and CIP treatment. In other words the POX process under normal conditions does not lead to gold dissolution (this is so because gold does nor form complexes with sulphate anions) as such but only to liberation, i.e. it is equivalent to a form of “chemical grinding”. In some instances, however, modification of the POX conditions involving the use of chloride or mixed sulphate/chloride media (instead of strictly sulphate) has been proposed in order to affect the dissolution of gold during POX processing, in this way avoiding the subsequent cyanidation step. In this case the soluble gold following POX is conceived to be recovered via CIP (carbon-in-pulp) by adding activated carbon to the discharged acidic slurry. This concept was originally described by Demopoulos et al. back in 1989 [47] and later by others [65]. A particular process variation of this direct solubilisation approach is the so-called PLATSOL process [66-68]. In this process gold and platinum-group metals-PGM (hence the origin of the name) are solubilised in the presence of 20 g/L (typically) chloride addition at 220 °C while all metal sulphides are oxidized to metal sulphates and sulphuric acid. The gold and PGMs form chlorocomplexes and stay in solution from which they are recovered after POX and solid/liquid separation by either adsorption or reduction processes. In this respect, this type of process differs from the approach investigated here as it does not involve the addition of carbon in the autoclave for direct recovery (during POX) of the gold chlorocomplexes.

2.8 PROCESSING OF COPPER-BEARING GOLD ORES-THE CESL PROCESS.

The high temperature total oxidation process described earlier for the processing of copper concentrates is essentially the same (from a gold recovery standpoint) with the POX process for refractory gold ores hence it will not be discussed further. Instead the medium-temperature (150 ^oC) type of copper pressure leaching process and in particular the CESL (developed by Teck) process [68-70] is described. The key ingredient of the process is the addition of 6-15 g/L chloride as catalyst to accelerate the leaching kinetics of chalcopyrite-the most common and difficult to leach copper sulphide mineral. It is interesting to observe here that despite the presence of this quantity of chloride ions in the CESL autoclave no dissolution or losses of gold have been reported. This may suggest that if any solubilization happens, it must be short-lived with gold reporting ultimately to the residue from which it is recovered. The generalized CESL process flowsheet is shown in Figure10. The feed, copper flotation concentrate, is sent to the pressure leaching autoclave. The copper sulphides are fully oxidized and the copper is solubilised. Any pyrite present reacts only partially because it is a highly “noble” mineral that forms a galvanic couple with chalcopyrite. The majority of oxidized iron reports in the residue as hematite and jarosite. At the same time elemental sulphur is the dominant sulphide oxidation product. A counter current S/L separation/washing circuit (CCD) separates the copper-containing solution and the gold-bearing solids. The copper-containing solution is sent to a copper recovery process (typically consisting of solvent extraction and electrowinning). The washed solids (which may have been previously separated from the elemental sulphur by flotation) are sent to another autoclave where they are subjected to pressure cyanidation [22,23] in order to recover gold by dissolution as soluble gold-cyanide complexes. The products from the second autoclave stage are sent to a carbon-in-pulp (CIP) circuit to recover the leached gold with activated carbon. The pulp is screened and the gold-loaded carbon is transferred to an elution circuit while the remaining pulp is sent to a cyanide destruction plant and subsequently disposed in a tailings pond. The activated carbon is eluted exactly as in the POX process and the gold cyanide solution (eluate) is electrowon to recover gold.

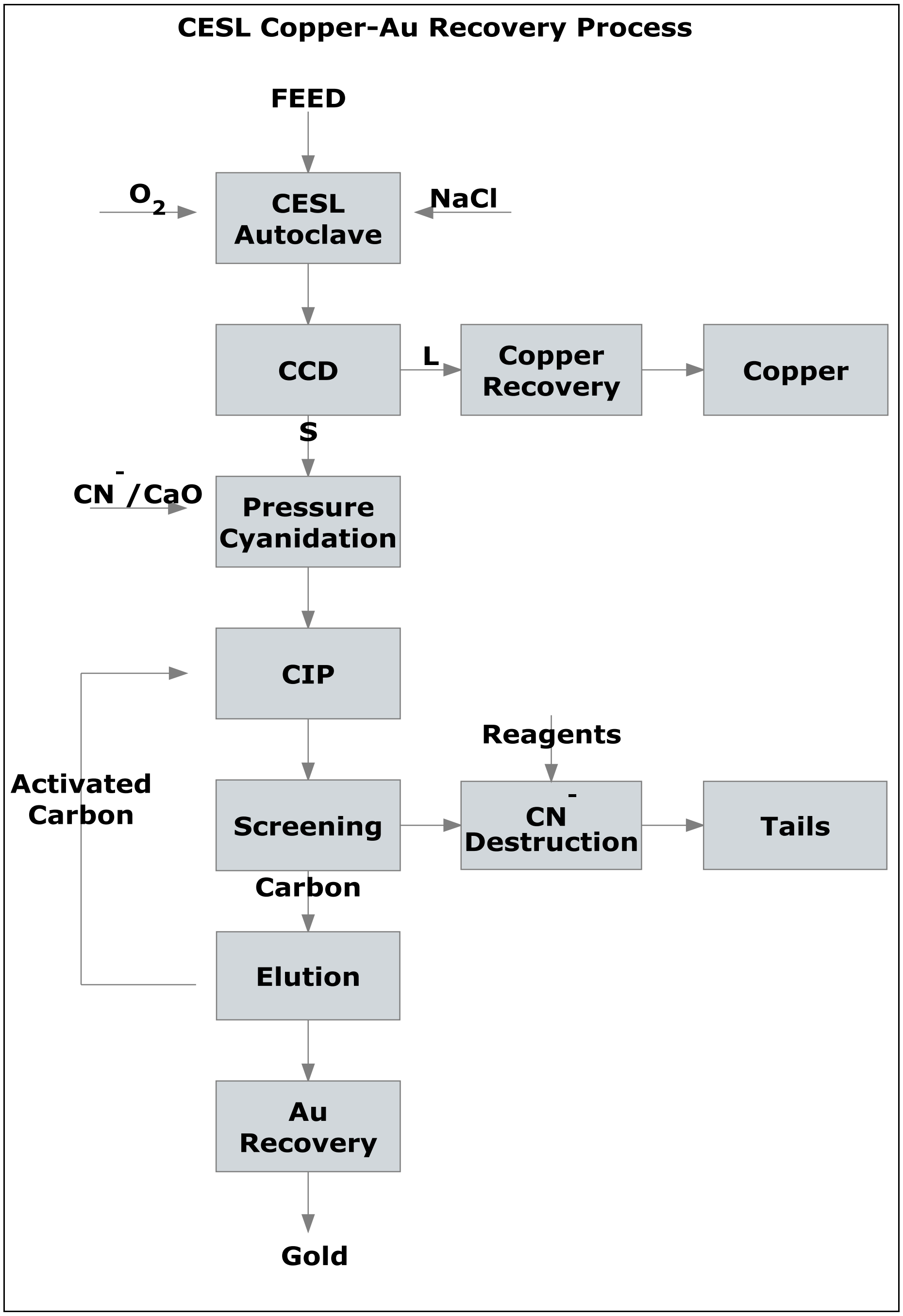

Figure 10: General CESL copper pressure leaching process flowsheet

Chapter 3. **METHODS AND MATERIALS**

This chapter describes the procedures employed as well as the reagents used.

3.1 CHEMICALS

Table 1: Information on chemicals used

CHEMICAL	FORMULA	SUPPLIER	ASSAY
Gold(III)chloride solution	$HAuCl_4$	Sigma Aldrich	17.5 % Au
Hydrochloric acid reagent grade ACS pure	HCl	Fisher Scientific	36.5-38%
Sulphuric acid reagent grade ACS pure	H_2SO_4	Fisher Scientific	95-98%
Nitric acid reagent grade ACS pure	HNO_3	Fisher Scientific	68-70%
AA Standard Au 1000 mg/L	$HAuCl_4$	Sigma Aldrich	17.5 % Au
Pyrite	FeS_2	Falconbridge mine	99%
Sodium chloride	NaCl	Sigma Aldrich	> 99.5 %
Sodium sulphate	Na_2SO_4	Sigma Aldrich	> 99.0 %
Activated carbon	$C_{(s)}$ (type GRC 20 12x30)	Calgon Carbon Corporation	100 %
Iron dust	$Fe_{(s)}$	Fisher Scientific	> 99.0 %

3.2 ATMOSPHERIC ADSORPTION EXPERIMENTS

All of the solutions had an initial gold concentration of 30 ppm (0.152 mmol/L) and pH of 1.5. This solution was prepared by mixing 15 mL of a 1 mg Au/mL gold chloride standard in 485 mL of distilled water. The pH was adjusted with sulphuric acid (95-98%, sulphuric acid concentration) and the chloride concentration using sodium chloride. In all solutions the molar ratio $[Cl^-]/[Au]$ was 5. The solutions, placed in 2 L Pyrex beakers were agitated at 300 rpm using a glass impeller and heated on a hot plate to the desired temperature, namely 20 ^oC (room T), 60 ^oC and 95 ^oC. The temperature was monitored via an electronic thermometer. Once the desired temperature attained, an initial solution sample was taken to verify the initial gold concentration followed with the addition of various amounts of activated carbon (Calgon type GRC 20 12x30) resulting in 0, 15 and 20 g/L activated carbon loadings (carbon was conditioned in a dilute HCl solution overnight). The solution was sampled (time 0,1,3,5,10,15 min) and filtered through 0.22 µm disposable PTFE filters. The resulting solution was sent to Atomic Adsorption Spectroscopy for elemental gold analysis.

3.3 AUTOCLAVE PRESSURE OXIDATION / CARBON ADSORPTION TESTS

Two titanium autoclaves were used for high pressure oxidation tests; both from Parr Instruments, a 2 L and a 300 mL titanium autoclave. In both titanium autoclaves a Pyrex liner was used. Despite, the use of the liner, significant plating of gold on immersed metal components as well as outside the solution and on the head and walls of the bomb occurred (lower part where solution condensed outside the liner)-refer to Figure 11. Various efforts were devoted in reducing the plating problem, including complete removal of the internal Ti-made parts in contact with the solution; like the impeller/stirring shaft and sampling tube. A solution to the plating problem was to coat the internal parts with Teflon, however none of these proved 100% effective. Thus finally a low pressure 300 mL glass autoclave (Parr Instruments Inc.) was chosen and used as viable alternative.

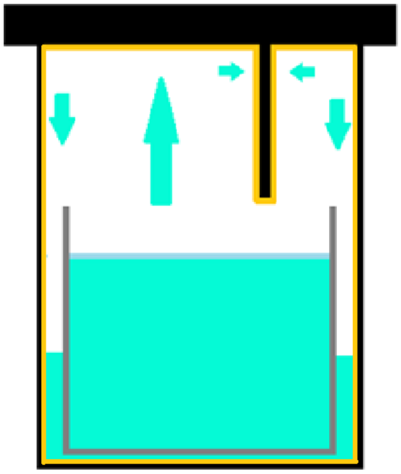

Figure 11: Schematic of autoclave and observed gold plating/deposition area

3.3.1 2 L Parr instruments titanium autoclave

The 2 L titanium autoclave consisted of titanium internal parts, such as a thermo well and stirring shaft/impeller, the cooling coil was removed as to minimize the exposed titanium surface within the autoclave. This autoclave was agitated at 300 rpm with a magnetic drive and 4-pitched blade titanium impeller, and heated with the complementary mantle from Parr instruments. However, this autoclave was set aside after a few tests since its metal impeller was prone to gold plating anf carbon attrition (the latter estimated at ~1%). As a replacement a 300 mL titanium autoclave, which had a Teflon-coated impeller was used instead since this reduced plating and formation of carbon fines.

3.3.2 300 mL Parr instruments titanium autoclave

The 300 mL autoclave was modified as first done by Blais [1]. Thus all titanium internal parts were removed and instead, agitation (using a 2 cm Teflon-coated magnetic stir bar) and heating were provided by a programmable hot plate as shown in Figure 12 (temperature was monitored via internal Teflon-coated thermowell). The thermo well was shortened to avoid dipping into the solution, hence minimizing the gold plating problem. Agitation was constant at 600 rpm.

Figure 12: Parr 300 mL titanium autoclave

3.3.3 300 mL Parr instruments glass autoclave

As mentioned already because of the experienced gold plating problem some tests were performed using a 300 mL glass autoclave like the one shown in Figure 13. The titanium internal parts such as the inner head and the thermo well were Teflon-coated (Canadan Coating Industries Ltd.) to minimize/eliminate plating. The heating was provided by a heating mantle, (not shown here) and the agitation was provided by a hot plate/stirrer and a 2 cm Teflon-coated magnetic stir bar.

Figure 13: Parr 300 mL Glass autoclave

3.3.4 Pressure oxidation procedure

The experimental procedure was identical for the 2 L and 300 mL titanium autoclaves, the only difference being the quantities of reagents used. The initial solution was prepared directly in the Pyrex liner. Firstly the gold chloride solution was prepared by mixing the required amount of gold chloride standard and deionized water. Then all gold was forced to precipitate via cementation using iron dust to mimic the refractory gold liberated during pressure oxidation. The solution was agitated manually for approximately 2 min before a liquid sample (1 mL using 0.22 μm disposable PTFE filters) was taken to ensure that all of the gold is in elemental form. Subsequently into this solution, the desired amounts of ground (d_{80} 38 μm) pyrite (mimicking the refractory sulphide mineral carriers), sodium chloride (as source of stoichiometric access chloride ions) and sodium sulphate (to promote formation of jarosite) were added. The solution was agitated manually for 1 min to allow for adequate mixing/homogenization and then the pH was adjusted to 1.5 using sulphuric acid. Finally into this solution activated carbon was added before the Pyrex liner containing the slurry was placed into the autoclave bomb. The autoclave was brought to the desired temperature (155 ^{o}C or 200 ^{o}C) while agitated at around 100 rpm during the warm up period (30-40 min). Once the target solution temperature was reached, the agitation speed was increased to 600 rpm. The reactor was not flushed with nitrogen since it was found experimentally that without a significant partial oxygen pressure, even at high temperatures, reaction kinetics are very slow. Therefore once the system had reached the desired temperature, oxygen was introduced (partial pressure of 10 atm for titanium autoclaves and 3 atm for glass autoclave) and pressure maintained constant during test. The system was allowed to react for 2 hours (except the tests evaluating the effect of time) at the target temperature.

3.4 CHEMICAL ANALYSIS

3.4.1 Solution analysis

The various solutions and slurries were sampled and filtered with 0.22 μm disposable PTFE filters (to capture possible carbon fines). The solutions were diluted to render the soluble gold content under 10 ppm. Calibration solutions of 0.5, 5 and 10 ppm dissolved gold were used to calibrate the Varian AA240FS fast sequential Atomic Absorption Spectrometer and a CanLab gold lamp at 267.6 nm was utilized to determine the gold content.

3.4.2 Oxidation product analysis

In order to ascertain the nature of gold reporting with the oxidation products (iron precipitates) a minute amount of residue (0.05 g) was dissolved in 10 mL of 3 M *aqua* *regia* and allowed to fully dissolve for 24 hours. Initially when hematite was the oxidation product the digestion period was much longer upwards of 2 days, however as an increasing amount of sodium was added to the oxidation mixture natrojarosite was produced, which dissolves much more readily. In addition to this in-house performed digestion analysis some residue samples were also sent to an external laboratory (Activation Labs in Lancaster, ON) to be analyzed for gold via neutron activation analysis. Characterization of the iron precipitate products was performed using XRD (Philips PW 1710 X-Ray diffractometer) and SEM (Hitachi S-3000N Variable Pressure Scanning Electron Microscope).

3.4.3 Gold-loaded activated carbon analysis

All of the gold-loaded activated carbon samples from the various atmospheric adsorption and pressure oxidation/adsorption experiments were sent to Activation Labs in Lancaster, ON to be analyzed via neutron activation analysis as the latter method provides reliable gold determination down to the ppb scale and for all other elements present down to the ppm scale [71].

3.5 XPS ANALYSIS OF GOLD-LOADED ACTIVATED CARBON

Gold-loaded activated carbon samples taken from atmospheric adsorption or pressure oxidation experiments were examined by scanning electron microscopy (Hitashi S-3000N) and analyzed via X-Ray Photoelectron Spectroscopy (XPS) in order to determine the exact mode by which gold loaded on carbon. However, due to the low gold content XPS analysis could not be performed. Thus it was decided to prepare highly loaded gold samples for XPS analysis by performing specially designed adsorption tests at 20 ^oC, 95 ^oC and 200 ^oC. The high-gold loaded carbon samples were prepared following the atmospheric adsorption experimental procedure; however in this case only 1 g of carbon was added to a 1 L solution (instead 15-20 g/L earlier used) containing 30 ppm of dissolved gold (as $HAuCl_4$, and having [Cl]/[Au]=5) and allowed to adsorb completely for 1h. In addition, a high Au-loading experiment was performed at 200 ^oC. In this case, a 0.5 L solution of 30 ppm dissolved gold was prepared and the gold was cemented out with iron dust. The pH was set to 1.5 and the chloride concentration was varied depending on the experiment. To this solution, 0.5 g of activated carbon was added and the solution was heated and allowed to react (equilibrate) for 2 hours, similar to the standard pressure oxidation test procedure but not having pyrite undergoing oxidation this time.

Chapter 4. CARBON ADSORPTION OF GOLD(III) CHLORIDE OVER HIGH TEMPERATURE

In this chapter the effect of temperature (over the range 20-95 ^{o}C) on the adsorption of gold(III) chlorocomplexes onto activated carbon is investigated. Emphasis is given on the kinetics of adsorption and the characterization of the “adsorbed” gold rather than the design of a carbon adsorption circuit. Previous work dealing with the adsorption kinetics of gold(III) chloride concerned room temperature adsorption only. Apparently, the effect of temperature on gold(III) chloride adsorption has not been studied previously other than some limited data reported by Avraamides et al. and cited as a reference in a publication by Hughes and Linge [62].

4.1 ADSORPTION OF GOLD(III) CHLORIDE

Following the procedure outlined in section 3.2 of Chapter 3, atmospheric adsorption experiments were performed with a solution containing 1.5 10^{-4} M Au(III) and 0.05 M chloride concentration (or 1 M in the high chloride series) at pH of 1.5. Tests were done at three different carbon loadings (10,20 and 30 g/L) and three temperatures, 20,60 and 95 °C.

4.1.1 Kinetic curves-parameter effects

The variation of soluble gold(III) concentration with time for the three different temperatures tested is shown in Figures 14, 15 and 16. As it can be seen complete gold removal was achieved within a few minutes of contact. The kinetics increases with increasing carbon loading as well as temperature. However an increase in chloride concentration from 0.05 M to 1 M was found to somewhat slow down gold adsorption as it can be seen with the data plotted in Figures 17 and 18. Sun and Yen [61] reported that increasing chloride concentration (up to 20 g/L, i.e. ~0.55 M) does not have a significant effect on adsorption kinetics, attributing this to the absence of competitive adsorption by chloride ions.

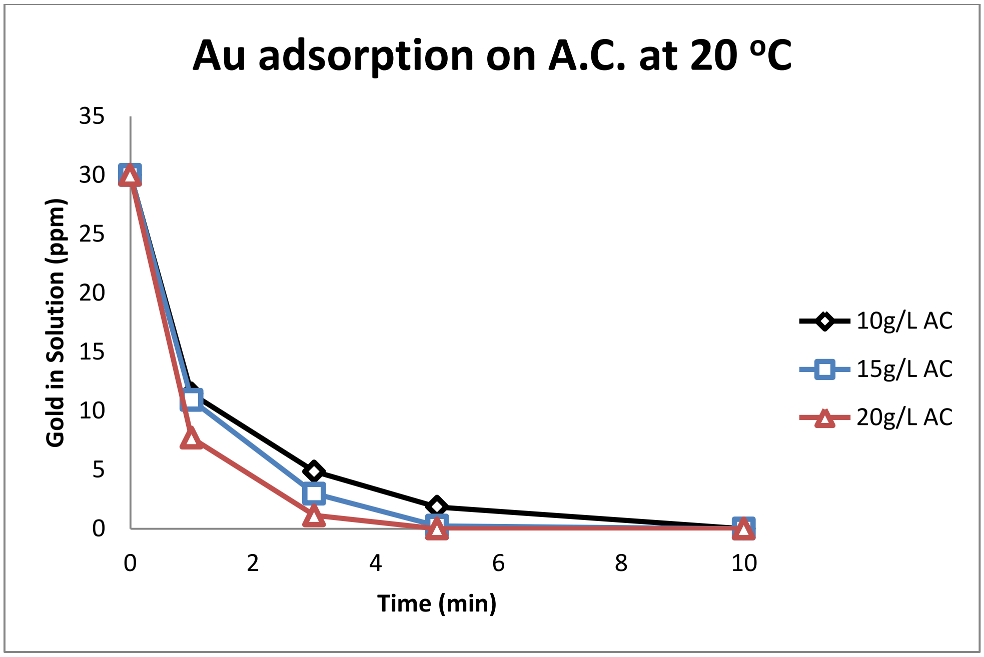

Figure 14: Adsorption kinetics of gold(III) chloride on activated carbon at 20 °C

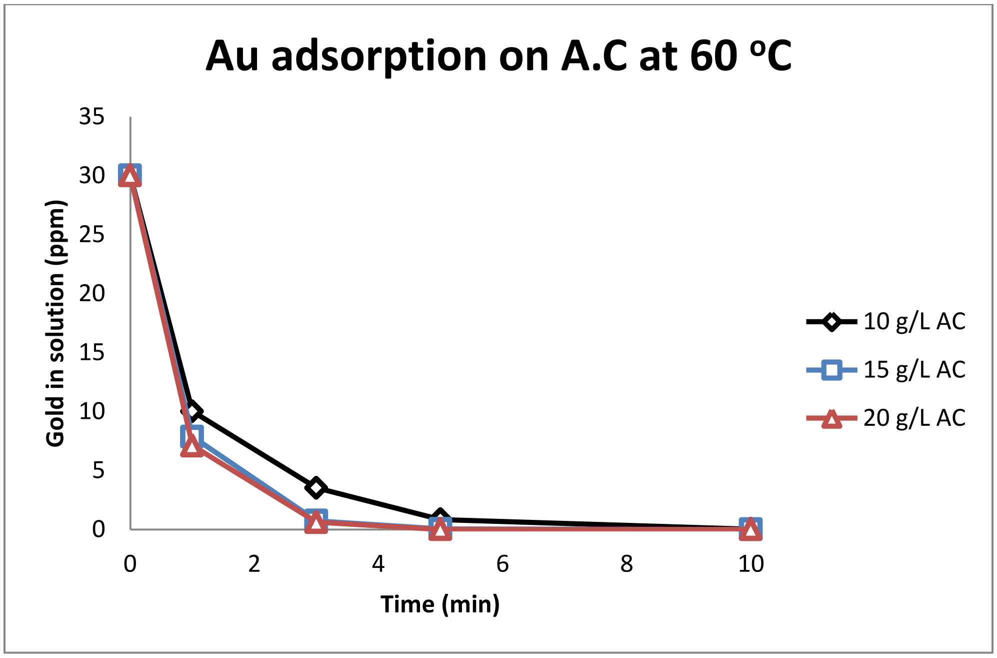

Figure 15: Adsorption kinetics of gold(III) chloride on activated carbon at 60 °C

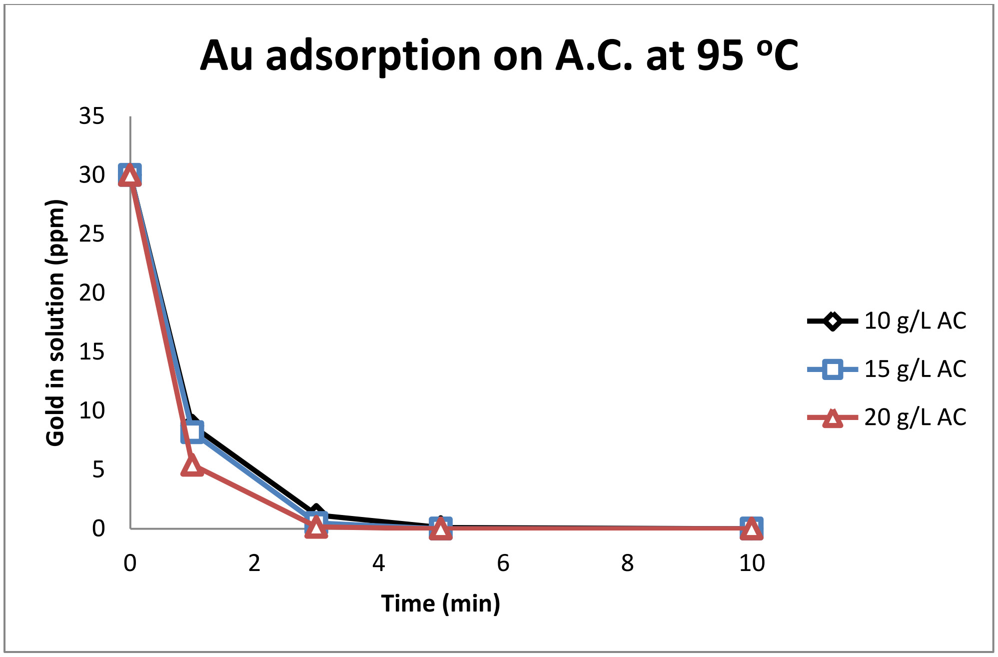

Figure 16: Adsorption kinetics of gold(III) chloride on activated carbon at 95 °C

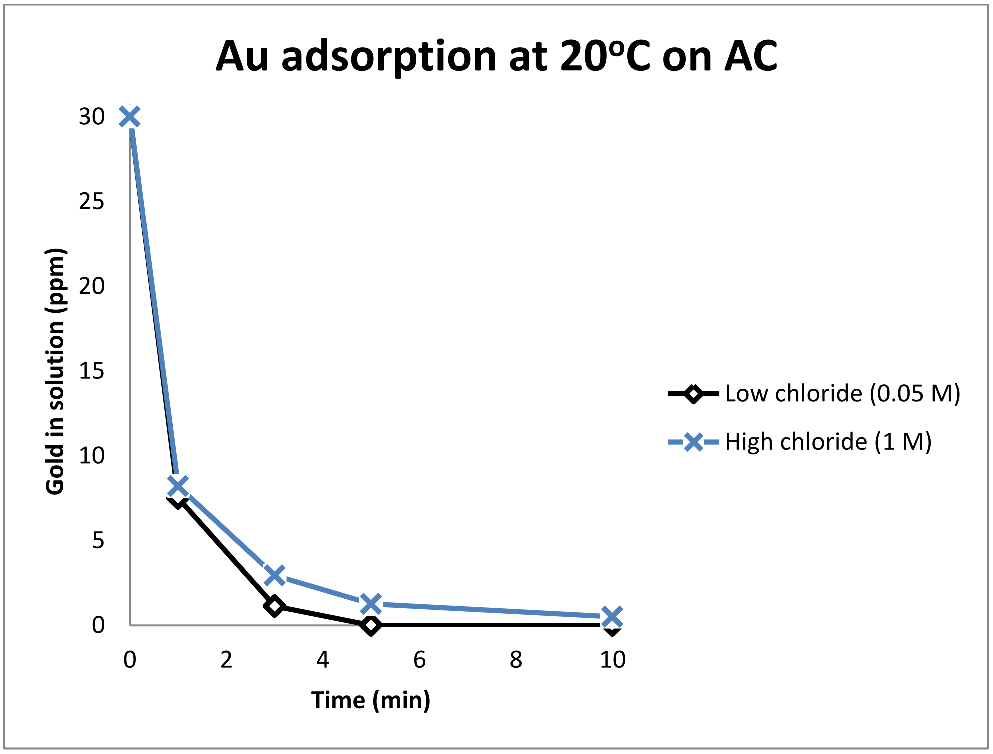

Figure 17: The effect of chloride ion concentration on gold adsorption kinetics at 20 °C using 20 g/L carbon loading

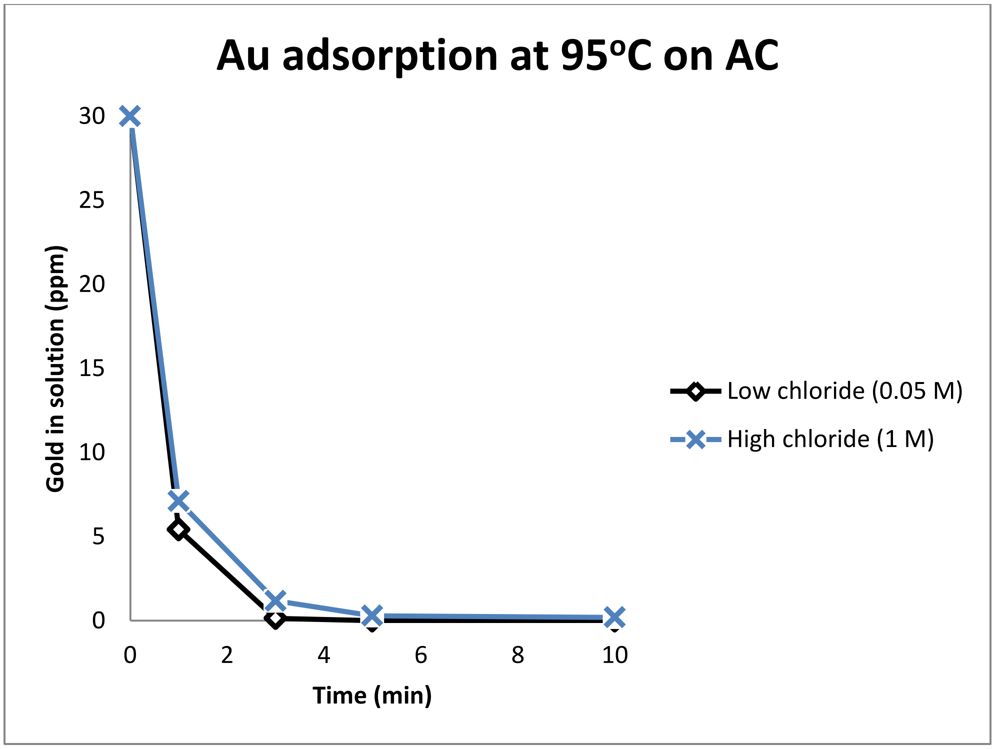

Figure 18: The effect of chloride ion concentration on gold adsorption kinetics at 95 °C using 20 g/L carbon loading

4.1.2 Kinetic analysis

Previous studies [61,62] found the kinetics of gold(III) chloride adsorption on carbon to be described by a first order rate law (as expressed by eq 14) and be diffusion-controlled.

$$[Au] = [Au]_o e^{-kt} \qquad (14)$$

Re-plotting the data of the C vs. t curves (Figs 14-16) according to the first order law as shown in Figures 19-21, linear plots were obtained as well in this work.

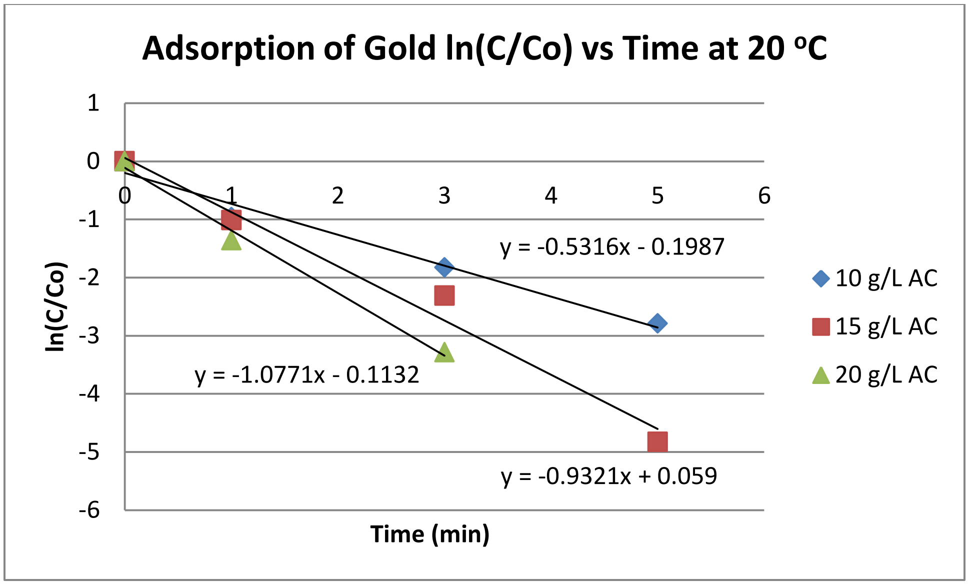

Figure 19: First-order adsorption kinetic plots at 20 °C

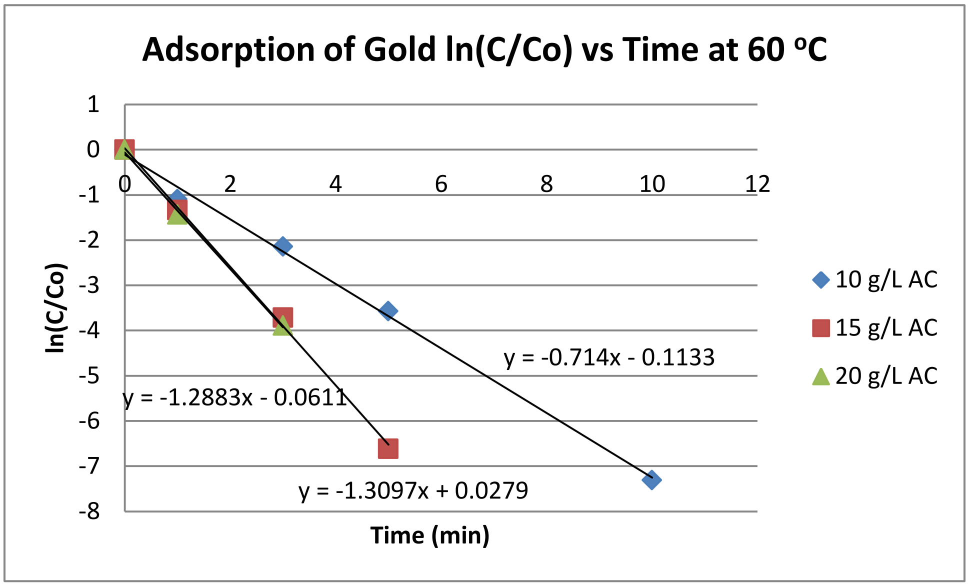

Figure 20: First-order adsorption kinetic plots at 60 °C

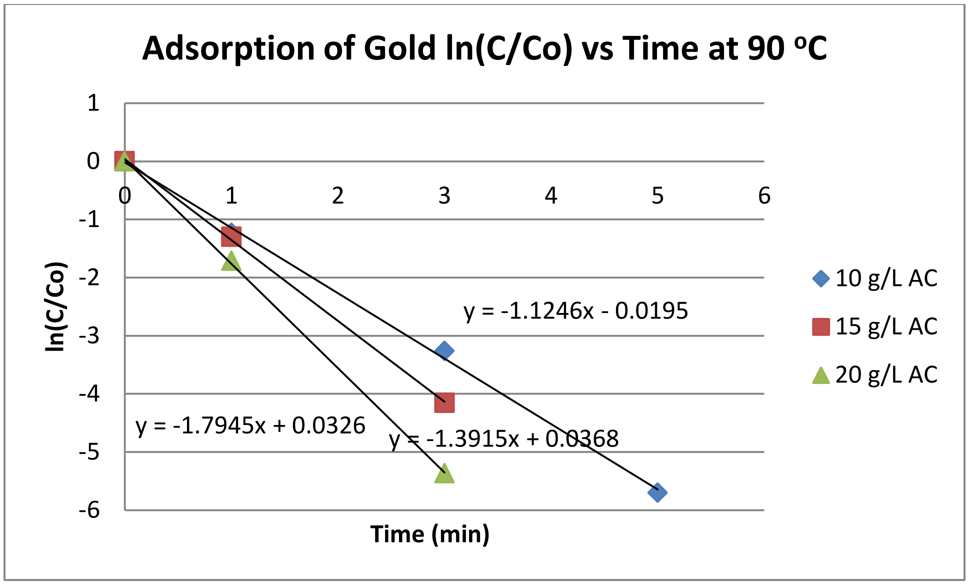

Figure 21: First-order adsorption kinetic plots at 95 ^{o}C

However, there was deviation from first-order behaviour at high chloride ion concentration. Thus as it can be seen in Figs 22 and 23 a change in the mechanism of gold adsorption after 5 minutes apparently occurs at high Cl^- concentration that needs to be further studied in more details in future work.

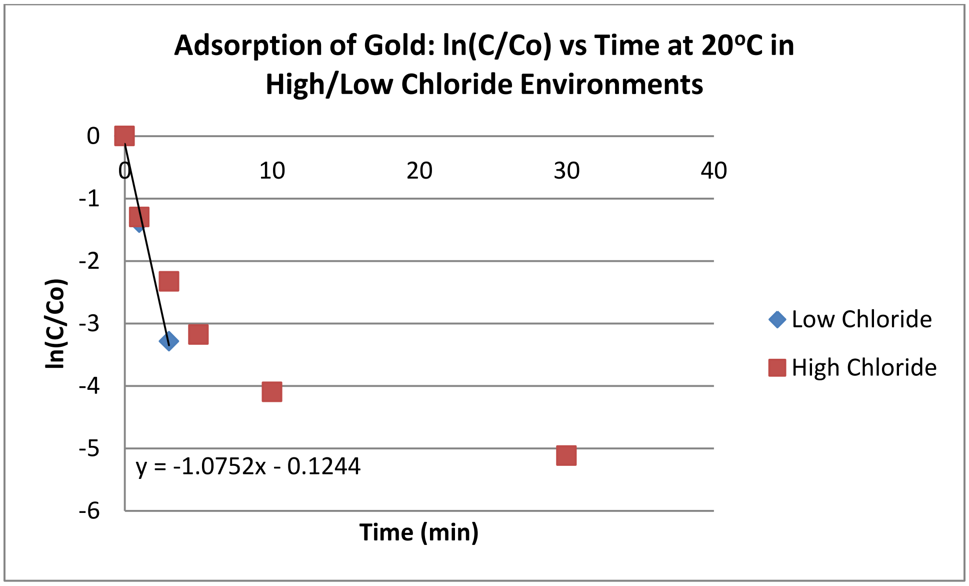

Figure 22: First-order adsorption kinetic plots-the effect of chloride ion concentration at 20 ^{o}C using 20 g/L carbon loading

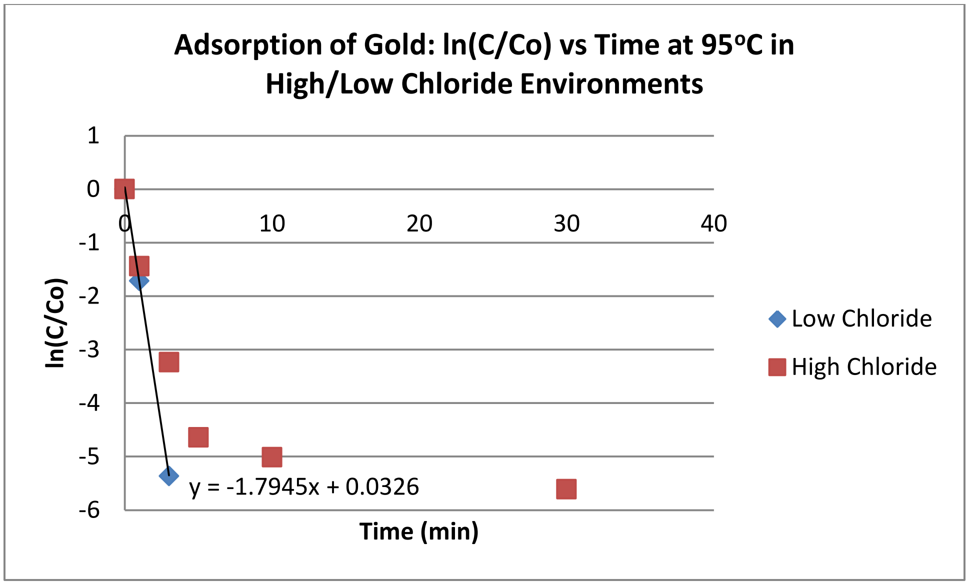

Figure 23: First-order adsorption kinetic plots-the effect of chloride ion concentration at 95 °C using 20 g/L carbon loading

Finally in order to evaluate the effect of temperature the linear plots (Figure 24) were re-plotted with the Arrhenius equation (15)(16) in the form of “ln(k)” (k, the rate constant) against 1/T (Figure 25). The Arrhenius plot yielded an activation energy of 8.69 kJ/mol. This value clearly points towards a diffusion-controlled process, this was also found in previous studies. The activation energy determined here is lower than the one cited in reference [62], which was 19 kJ/mol, but still within the range of activation energies for mass-transport controlled processes.

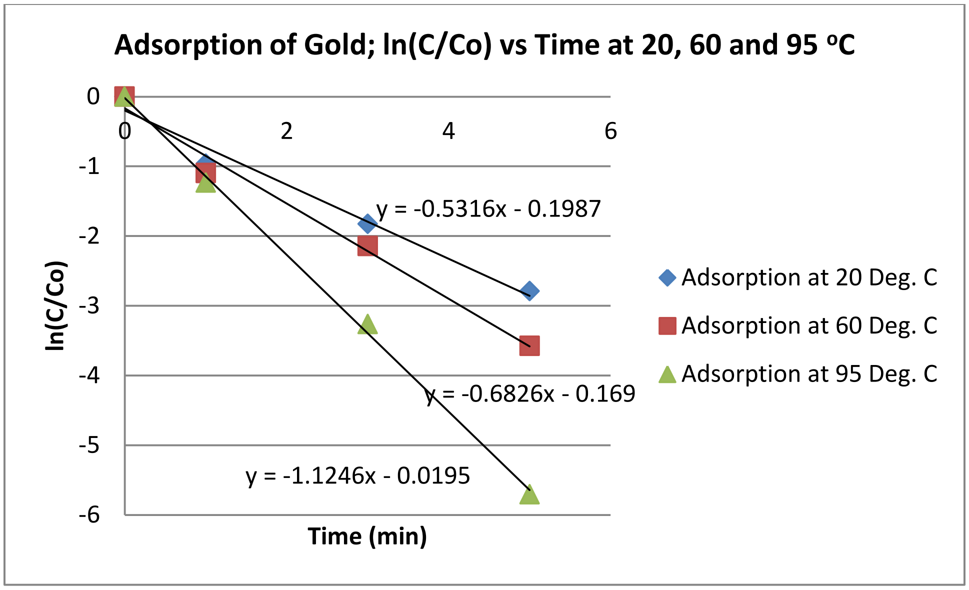

Figure 24: First-order adsorption kinetic plots (10 g/L carbon) at 20, 60 and 95 ^{o}C

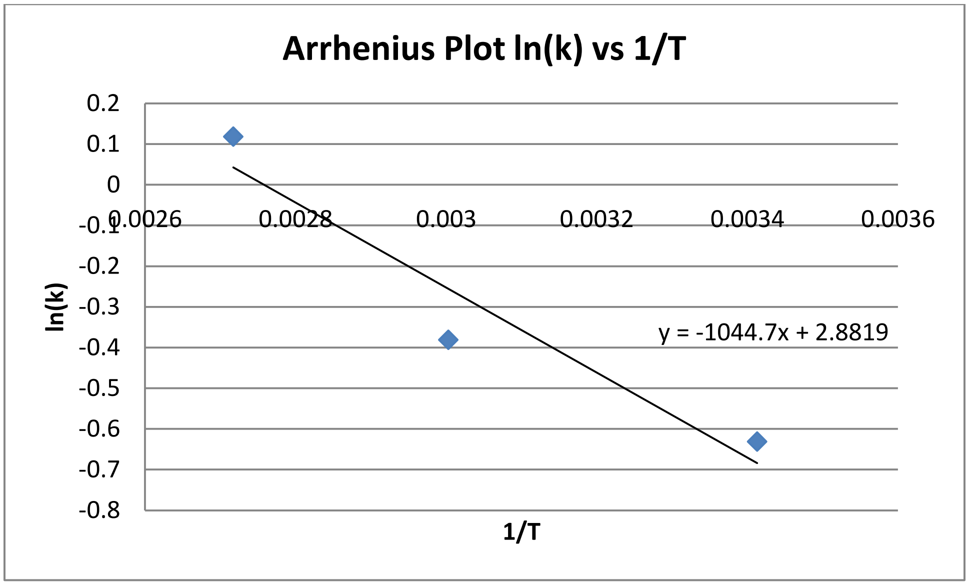

Figure 25: Arrhemius (ln(k) vs 1/T) plot (data from Figure 24)

$$k = Ae^{\frac{-E_a}{RT}} \tag{15}$$

$$ln(k) = ln(A) - \frac{E_a}{RT} \tag{16}$$

4.2 XPS OF GOLD-LOADED ACTIVATED CARBON

It was established in section 4.1 that gold chloride does adsorb readily on activated carbon even at 95 °C but the question remained as to in what form, [i.e. Au(I or III) complex or metallic gold] does it occur. In order to answer this question gold(III) chloride-carbon loaded samples were prepared at different temperatures as described in section 3.5 of Chapter 3 and analysed by X-ray Photoelectron Spectroscopy (XPS) as this method offers quantitative surface chemical analysis and speciation information.

First metallic gold was analysed in order to serve as reference material. XPS identification of metallic gold is indicated by its two characteristic peaks reported at values of 84.0 and 87.7 eV [72]; these peaks correspond to the $4f_{7/2}$ and Au $4f_{5/2}$ states. This was confirmed in the present work by analysing a metallic gold powder specimen as shown in Figure 26.

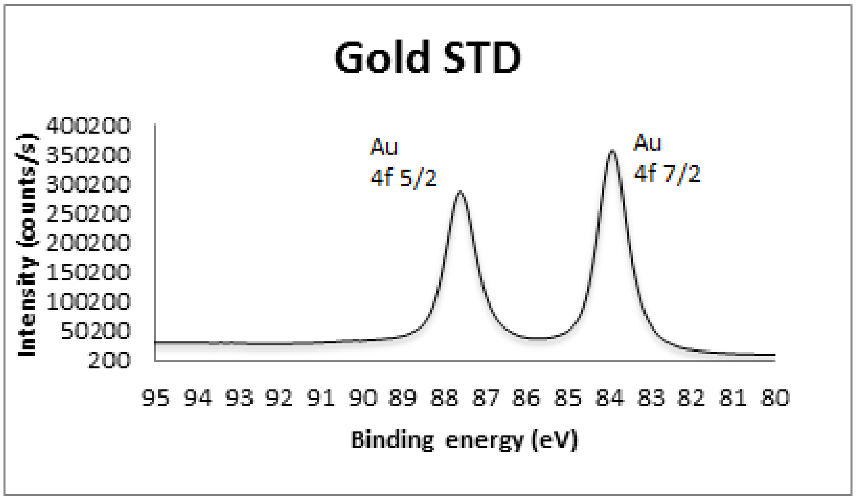

Figure 26: XPS spectrum of metallic gold standard

The previous XPS spectrum (Figure 26) is the original unfitted scan as are the XPS spectra that follow (Figures 27-30). These serve to to obtain a qualitative analysis of the changes occurring as a function of temperature (20 vs. 95 °C) as well as at low (0.05M) and high (1M) chloride concentration. However, it should be noted that all XPS spectra presented here were de-convoluted to obtain quantitative results of the amount of each gold species present as shown later in Table 2.

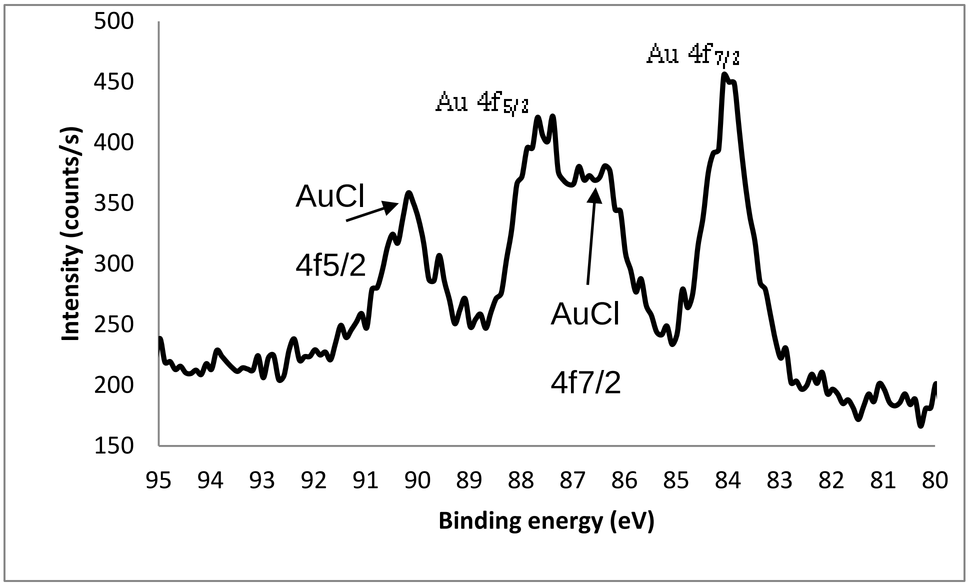

Figure 27: XPS spectrum of gold loaded on activated carbon at 20 °C with low chloride concentration (0.05M)

Figures 27 and 28 show the spectra of the gold-loaded activated carbon obtained via adsorption at room temperature conducted with low (0.05M) or high (1.0M) chloride concentration. In these spectra it becomes apparent that there are more peaks than the two corresponding to metallic gold (Figure 26). Thus in this case we note the presence of two secondary peaks at 90.4 and 86.4 eV in addition to the two (at 84 and 87.7 eV) of metallic gold. These extra gold surface states observed also in previous works [72] have been correlated to being the valence states of Au(I), which is on the surface of the carbon in the form of AuCl. Indeed the values obtained experimentally in this work correspond closely to the literature values listed at 86.1 and 89.9 eV [72]. The presence of a Au(III) state (appearing at ~ 87 and 91 eV [72] was not observed at all. There were not distinctive differences between the low and high chloride systems (Figures 27 and 28).

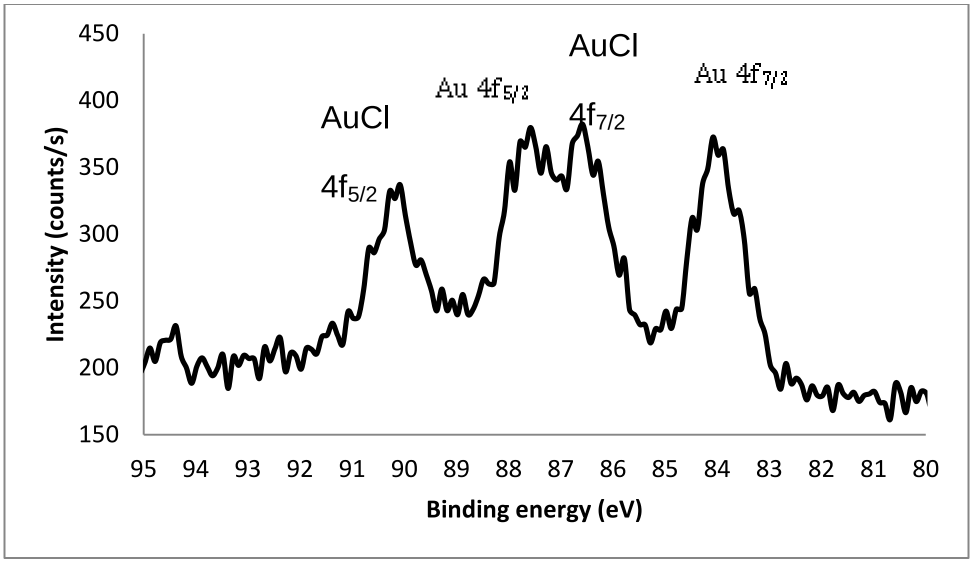

Figure 28: XPS spectrum of gold loaded on activated carbon at 20 ^{o}C with a high chloride concentration (1M)

The corresponding spectra at 95 ºC are shown in Figures 29 and 30. At this temperature, the doublet peaks corresponding to Au(I)Cl (AuCl $4f_{7/2}$ and AuCl $4f_{5/2}$) have diminished, corresponding to an increase in metallic gold species. This phenomenon is observed equally at low and high chloride concentrations indicating that reduction to metallic gold if favoured at higher temperatures, an observation consistent with thermodynamic calculations reported by Blais [1]. XPS analysis was also done for carbon samples from the autoclave pressure leaching tests at 200 ºC (reported in section 5.3.5 of the next Chapter), where again similar gold loading characteristics were noted.

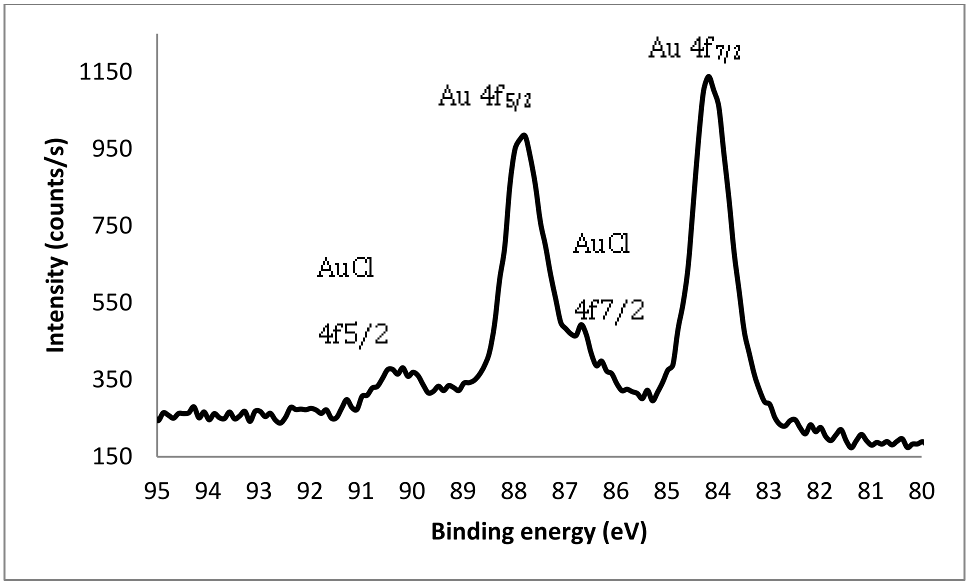

Figure 29: XPS spectrum of gold loaded on activated carbon at 95 ^{o}C with low chloride concentration (0.05 M)

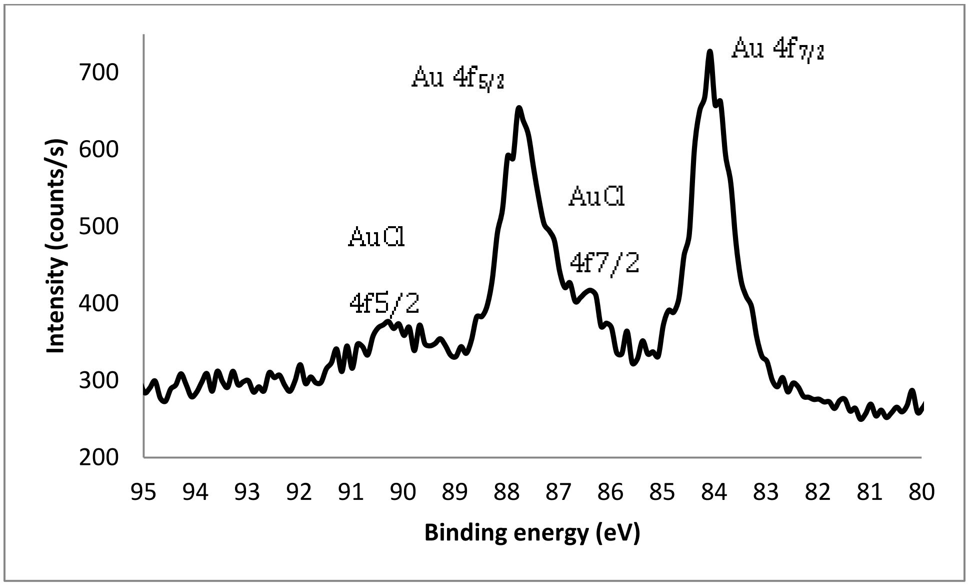

Figure 30: XPS spectrum of gold loaded on activated carbon at 95 ^{o}C with a high chloride concentration (1 M)

Previous research [72] has demonstrated that at room temperature, ~40% of the gold adsorbed on activated carbon is in the aurous form. By the integration of the area under the peaks characterizing the Au(0) (Au 4f $_{7/2)}$ and Au(I) (AuCl 4f $_{7/2}$) states the relative amount of each species was determined. The obtained results are summarized in Table 2. As it can be seen at room temperature 45-50% of gold loaded on carbon was in the form of AuCl not far from the 40% value previously reported [72]. As the temperature increased the amount of Au(I) decreased, while as the chloride ion concentration increased there was an increase in Au(I) complex presence. These trends are consistent with the relative stability of the Au(I)-chlorocomplex [73]:

$AuCl \rightarrow Au^{1+} + Cl^{-1}$

$Au^{1+} + e^{-} \rightarrow Au$

Table 2: Distribution of gold species on carbon according to the area of integration under the Au(I) (4f 7/2 at 84 eV) and Au(s) (Au 4f 7/2) XPS peaks

	LOW CHLORIDE		HIGH CHLORIDE	
Temperature	**Au(I)**	**Au(s)**	**Au(I)**	**Au(s)**
20 °C	45 %	55 %	50%	50%
95 °C	34%	66%	38%	62%
200 °C	30%	70%	33%	67%

Chapter 5. CARBON-IN-AUTOCLAVE

In this chapter the tests performed involving carbon addition in autoclave in order to evaluate the extent of in-situ gold recovery in a simple pressure oxidation-leaching system are described and discussed. In a typical carbon-in-autoclave test a simulated "refractory" feed material was used consisting of ground pyrite as model sulphide mineral along with metallic gold deposited in the starting slurry by cementation. The starting solution contained as well different amounts of free chloride and sodium ions. Details on experimental solution compositions and procedures employed are described in Chapter 3. The presence of adequate chloride and sodium ion concentrations was required to ensure the solubilisation/adsorption of gold and suppression of hematite formation. The presence of sodium favours the formation of jarosite instead of hematite thus avoiding the losses of gold due to adsorption on the latter. The differentiation in terms of gold chlorocomplex adsorption and therefore loss on hematite but not jarosite was studied/quantified in a recent study completed at McGill by Derek Blais [1]. The atmospheric carbon adsorption tests described in Chapter 4 provided the basis for the high temperature oxidation/adsorption tests described in this Chapter.

5.1 INITIAL SCOPING EXPERIMENTS

The conditions and results from the first series of tests are summarized in Table 3. In this series of tests a 300 mL capacity titanium Parr autoclave, with a Pyrex liner, was used. The Pyrex liner was required to avoid the loss of gold by plating/cementation on the metallic titanium surfaces. To minimize further gold losses (due to cementation) all internal metallic parts, including the stirrer[1], were removed as per findings reported by Blais [1]. Tests were conducted at two temperatures corresponding to the medium (CESL) and high temperature (POX) processing options. In tests 1 to 5 the oxygen partial pressure was 10 atm. In each test 75 mL of solution was used in which variable

---

[1] These tests serve only to study the behaviour of mobilized gold within the autoclave if activated carbon is present and provide "proof-of-concept" as fat it concerns the potential for direct gold recovery in autoclave. It is far from being a "process" especially given the fact that not real conditions, such as high slurry densities and aggressive agitation were employed, which may very well compromise the integrity of carbon leading to fragmentation and unacceptable losses.

amounts of Na_2SO_4 and NaCl were added along ground (80% -38µm) pyrite mineral and microscopic gold (30 mg Au/L added as $HAuCl_4$) precipitated in-situ by cementation with iron dust (0.05 g) to mimic a gold-carrying sulphide feed. Before heating up (30 min) the contents to target temperature, a fixed amount of activated carbon was added into the slurry as well. Once the target temperature was reached, oxygen was supplied to the autoclave and oxidation was allowed to take place for 2 hours, after which the solution was quickly cooled and immediately screened with a sieve of 80 micron size. The solution was analyzed for gold; the final residue (oxidation product) was digested in *aqua regia*, and then analyzed to determine its gold content (loss). The activated carbon was analyzed via neutron activation, which yields results in the ppb scale.

Table 3: Summary of results from initial pressure oxidation experiments

	TEST 1	TEST 2	TEST 3	TEST 4	TEST 5
CONDITIONS					
Ground Pyrite (g/L)	53.3	53.3	53.3	53.3	53.3
Activated Carbon (g/L)	40	40	40	40	40
Gold (mg/L)	30	30	30	30	30
Sodium[1] (g/L)	8.5	6.8	8.5	10.2	4.3
Chloride (g/L)	2.5	2.5	2.5	5	5
Temperature (^oC)	155	155	200	200	200
Pressure (atm)	10	10	10	10	10
Initial pH	1.5	1.5	1.5	1.5	1.5
Time (h)	2	2	2	2	2
Jarosite seed (g/L)	0	6.7	0	0	0
RESULTS					
Gold left in solution (%)	2.9	3.2	4.4	2.6	3.6
Gold lost in residue (%)	**18.9**	**1.9**	**3.2**	**0**	**21.8**
Gold Recovered on Activated Carbon (%)	**37.8%**	**64.6%**	**70.2%**	**75.6%**	**46.6**
Unaccounted gold[2] (%)	40.4	30.3	22.2	21.8	28

[1] This is total sodium including sodium sulphate and sodium chloride additions.
[2] Assumed to have plated on metallic surfaces inside the autoclave; this assumption is verified in the next series of tests.

Upon review of the results summarized on Table 3, it can be seen that there was partial reporting of gold on activated carbon varying from 37.8% (Test 1) to 75.6% (Test 4). Test 1, performed at 155 ^{o}C, was associated with about 20% of the gold remaining with the residue. Of the remaining gold, 3% was in solution and only 38% was recovered ("captured") by the activated carbon. Some 40% was unaccounted for. This "unaccounted" type of gold was thought to have been partially lost during sample handling and analysis but the majority to have "plated" on internal autoclave surfaces-a hypothesis verified later in the next series of tests. Interestingly the solution (approximately 40% of the total), that collected outside the liner due to evaporation and subsequent condensation upon cooling as per schematic shown in Figure 11 of section 3.3 and Figure 35 (A) of section 5.2, carried no soluble gold at low chloride concentration[2].

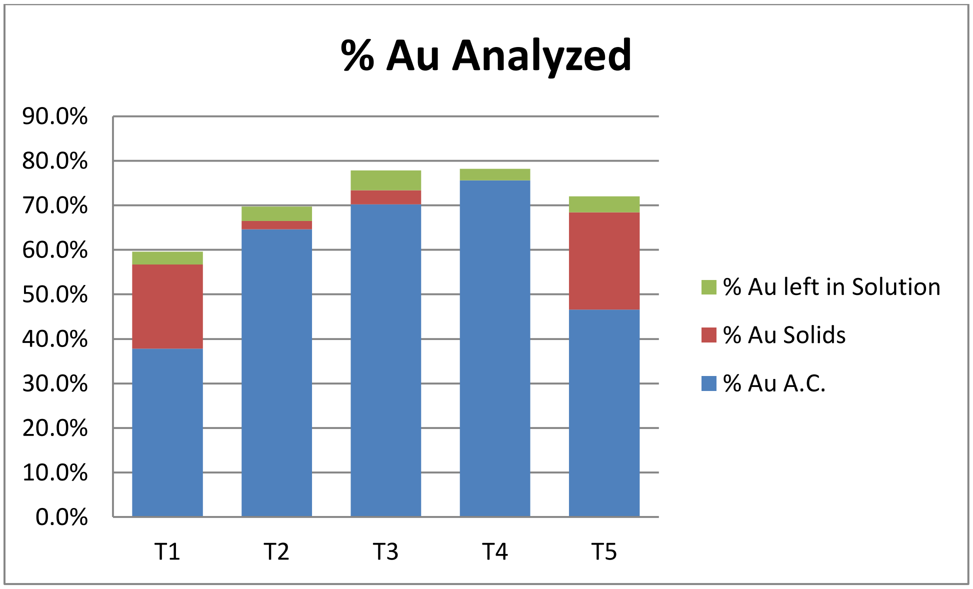

Figure 31: % Gold distribution at the end of C-in-autoclave experiments-series 1 (Table 3)

Effect of jarosite formation/seeding: The distribution of gold at the end of each of the first five experiments summarized in Table 3 is illustrated in Figure 31. The 20% of gold that reported with the residue in Test 1 was attributed to gold coprecipitation with the iron oxidation residue. As shown by Blais [1], gold(III) chloride adsorbs on hematite (but

---

[2] This was true for this series of tests carried with low chloride concentrations. Increased chloride concentrations (discussed in a subsequent section) resulted in transfer of some soluble gold chloride in the liquid trapped between the bomb and liner.

not on jarosite) hence it was thought in this case that inadequate jarosite formation was responsible for the 20% gold coprecipitation. The homogeneous precipitation of jarosite is known to be slow characterized by certain induction period. Seeding is known to accelerate jarosite kinetics [43]. Thus a new test was carried out this time in the presence of small amount of jarosite seed (Test 2). As seed sodium jarosite prepared as described by Dutrizac and Kaiman [44] was used. This time the amount of gold lost to the residue was indeed suppressed down to 2% only hence proving the importance of seeding, in particular during pressure leaching at the lower temperature range (~150 °C). Gold recovery on carbon now improved to ~65% with "unaccounted" gold being 30%.

Effect of temperature: Test 3 was identical to Test 1 except that the temperature had been raised from 155 to 200 ^{o}C. This time gold recovery on carbon increased to 70% despite the elevated temperature. This indicates an endothermic mechanism behind gold "adsorption" on carbon, i.e. a similar behaviour with that observed over the temperature range 22-95 ^{o}C in Chapter 4. This behaviour is the opposite of that exhibited in conventional gold adsorption practice that involves gold-cyanide complexes, where elevated temperatures are known to promote de-sorption. This observation proves that the mechanism is not based on physisorption but rather on a endothermic chemical reaction that as shown in the XPS characterization section of Chapter 4 leads to reduction of gold(III) into gold(I) and metallic gold. Interestingly enough gold loss in the residue was again limited to 3% but 22% of gold remained "unaccounted" meaning that deposited on internal autoclave surfaces as demonstrated later.

Effect of chloride concentration: Test 4 was run at a higher chloride concentration of 5g/L compared to 2.5g/L for Tests 1, 2 and 3. The chloride concentration was increased as pre-caution against reduction of gold chlorocomplexes to metal that is favoured with temperature elevation as explained on the basis of thermodynamic calculations by Blais [1] and discussed briefly in Chapter 2. In addition the amount of sodium (as Na_2SO4) was increased to 10 g/L to ensure that all iron precipitates as jarosite as in the previous test (no 3) a small amount of (undesirable) hematite had been noticed by XRD analysis (Figure 32).

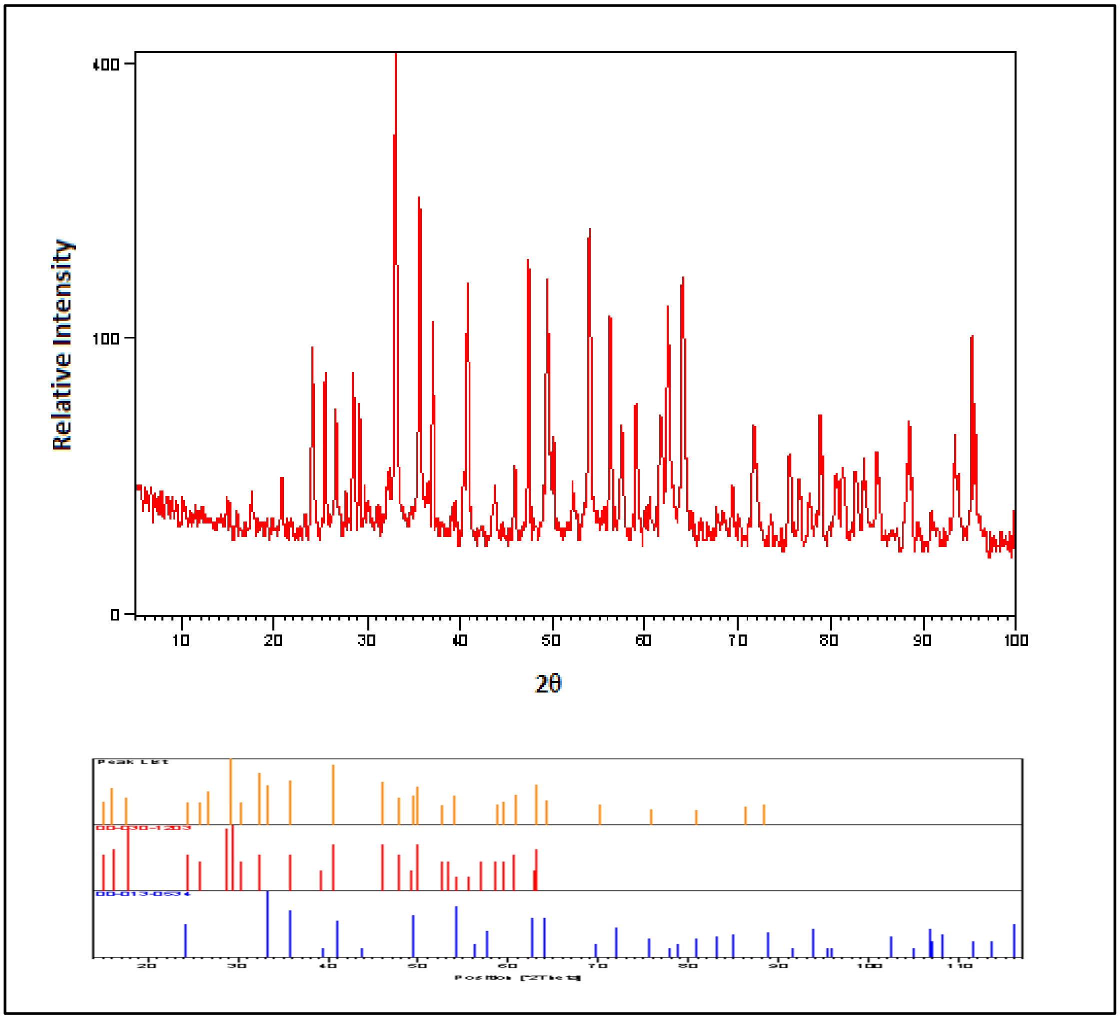

Figure 32: The XRD spectra above is the oxidation product of Test #3 from Table 3; Below the oxidation product XRD pattern (yellow peaks) compared to reference patterns (red peaks = natrojarosite, bleu peaks = hematite)

This amount of sodium (10g/L) corresponds to 3 times the iron concentration in solution (assuming 100% oxidation of pyrite). The complete oxidation of pyrite yielded quasi pure jarosite (Figure 32), with no gold lost in the jarosite residue. The corresponding amount of gold recovered on carbon this time was 75%.

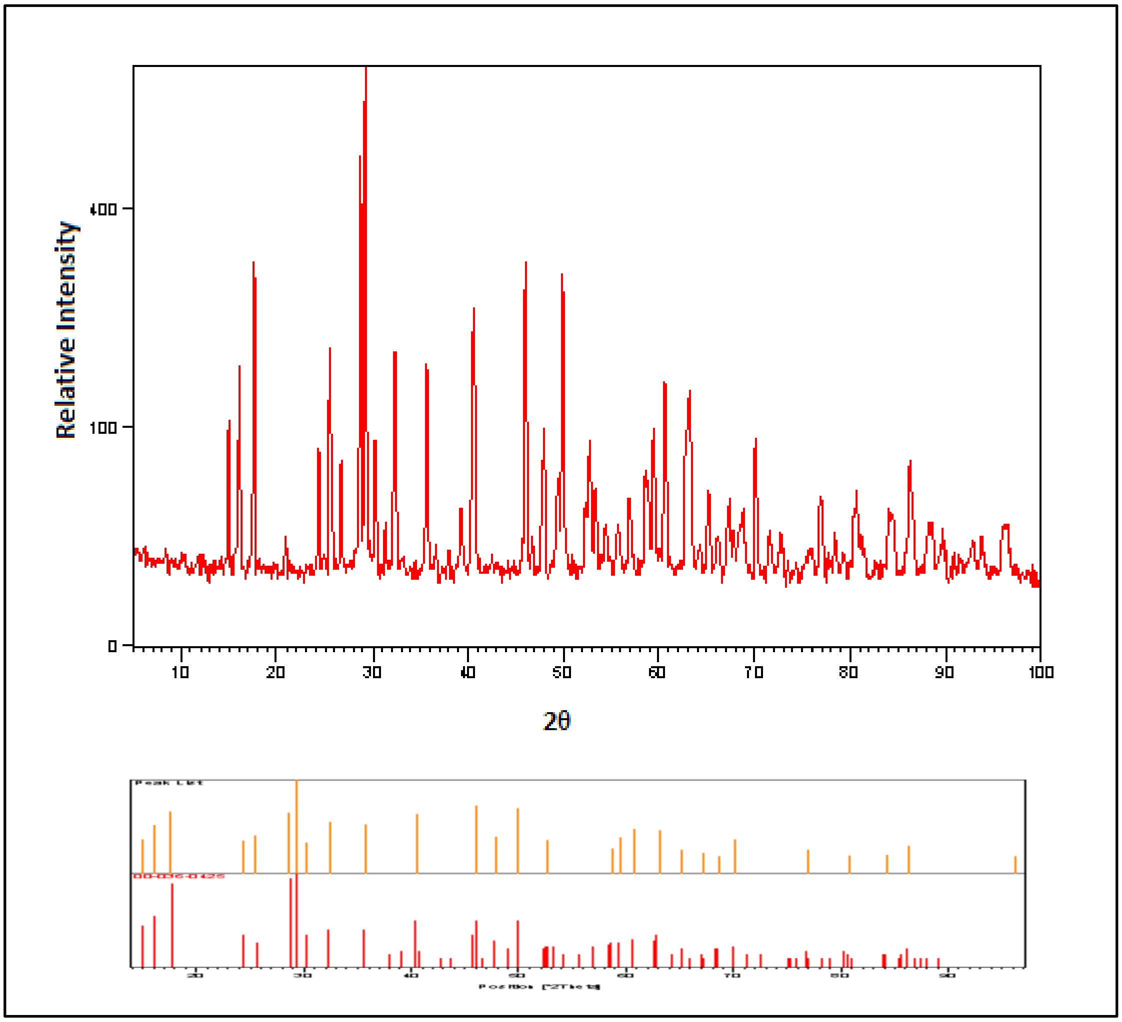

Figure 33: The XRD spectra above is the oxidation product of Test # 4 from Table 3; Below the oxidation product XRD pattern (yellow peaks) compared to the reference pattern of natrojarosite (red peaks)

Effect of sodium concentration: The importance of maintaining a high sodium concentration to favour the formation of jarosite (at the expense of hematite) is demonstrated with Test 5, where a smaller sodium concentration was used (4.25 vs. 10 g/L). This time a significant amount of gold accompanied the residue, namely 22% loss and the gold recovered on carbon was reduced to 46%. Apparently pyrite and gold were completely oxidised but the partial formation of hematite due to the inadequate amount of sodium led to gold losses via adsorption/coprecipitation with the former. In other words hematite formation causes a “preg-robbing” effect. The adsorption of gold(III) chloride at the surface of hematite has been described in literature [54] and observed/studied in our laboratory [1]. The beneficial effect of jarosite formation on gold recovery by carbon is rather counter-intuitive as in the pressure oxidation literature and practice [1,44,47,74] the formation of jarosite is known to cause the loss of silver. Although it is premature to talk of a process as such, it should be pointed out that in case of application, the use of a high concentration of sodium does not constitute a waste as the solution in an actual process can be at least partly recycled back into the autoclave.

Reproducibility: The favourable effect of jarosite formation (Figure 33) is further illustrated with the data of Table 4 and figure 34 below. In this series the same conditions as Test 4 from Table 2, were applied (53.3 g/L pyrite, 40 g/L carbon, 10 atm O_2, 200 ^oC, 5 g/L Cl^- but the amount of sodium was progressively increased from 6.8 to 10.2 g/L. More than one test was run for each sodium concentration in order to ascertain the quality/reproducibility of the data. The results in terms of gold distribution at the end of each test are summarized in Table 4. It can be seen once more an increase in sodium led to increased gold deportment on carbon due to the apparent formation of jarosite at the expense of hematite. Further the tests can be seen to be highly reproducible. Nevertheless the problem of gold plating (discussed below) persisted.

Table 4: Reproducibility results-the effect of sodium ion concentration

ID ON FIGURE 34	% AU LEFT IN SOLUTION	% AU IN RESIDUE	% AU ON CARBON	% AU PLATED	SODIUM CONCENTRATION (G/L)
1	2.76%	2.60%	38.61%	56.03%	6.8
2	3.32%	3.70%	46.96%	46.02%	6.8
3	2.54%	0.80%	57.26%	37.90%	8.5
4	2.96%	0.30%	63.78%	31.46%	8.5
5	2.86%	0.00%	62.35%	33.29%	8.5
6	3.35%	0.00%	65.22%	29.93%	8.5
7	4.45%	0.00%	66.52%	27.53%	8.5
8	4.06%	0.00%	65.35%	29.09%	8.5
9	4.72%	0.00%	72.26%	21.52%	10.2
10	4.84%	0.00%	73.96%	19.70%	10.2
11	4.23%	0.00%	68.61%	25.66%	10.2

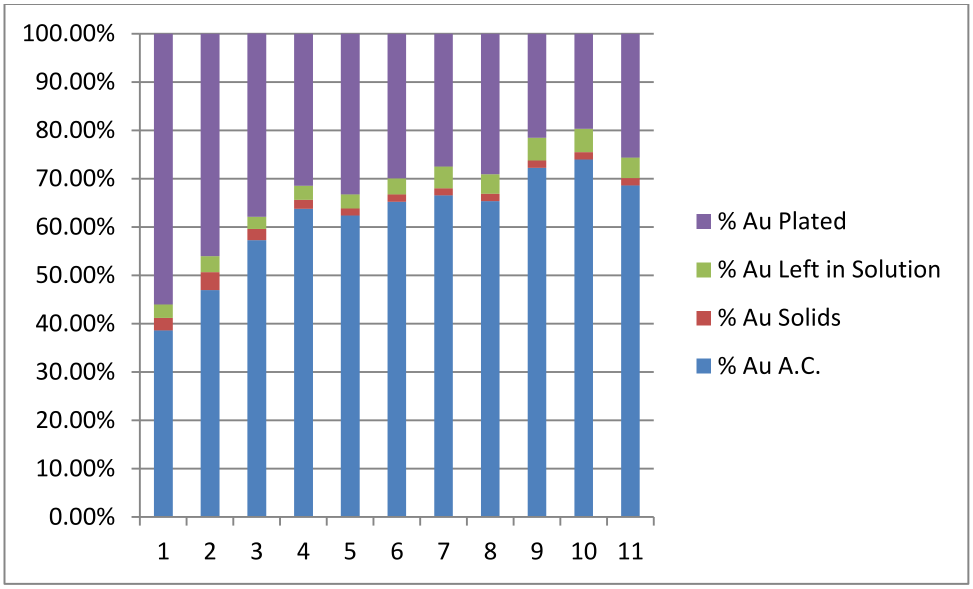

Figure 34: % Gold distribution at the end of C-in-autoclave experiments-the effect of sodium concentration (duplicate series)

Gold plating on metal surfaces: As noted above a significant amount of gold (20-30%) was “unaccounted”, i.e. was neither found to be on the carbon, in the solution or in the precipitated residue. This “unaccounted” gold was assumed to have plated out of solution on internal autoclave surfaces via electrochemical coupling similar to cementation reactions, an observation made also by Blais [1] and verified later in this Chapter. Assuming this to be the case this “plated” gold is not considered a permanent loss but only a temporary one. First of all industrial POX/PL autoclaves are brick lined and as such should be free of such cementation behaviour. Impellers that are currently made of titanium will have to be made of ceramic (not metallic) materials to cut down on the cementation occurrence, if carbon-in-autoclave use is contemplated. In addition industrial autoclaves are shut down on a regular basis (every few months) for the purpose of re-lining and maintenance. Such shut down will give the opportunity to recover any “plated” gold on internal surfaces via batch chloride leaching under oxygen overpressure, although such gold “lock-in” for several months may simply not be acceptable. At the conceptual level given the lower capital and operating costs associated with the single-step Carbon-in-autoclave system and the great benefit of not relying on cyanide the attractiveness of the new system become obvious.

Notwithstanding the option of recovery of any plated gold during the shutdown/maintenance of the autoclave, it is highly likely in tests with clean and larger autoclaves the occurrence of “unaccounted” gold (i.e. gold presumed to have plated on metallic surfaces inside the autoclave) not to be observed. (The particular Ti autoclave used for Tests 1 to 5 was an old vessel (circa 25 yrs old) having over the years been contaminated with various metallic and scale deposits that may have contributed to the observed losses).Thus in the similar systems of the CESL and PLATSOL process (where chlorides are added in the autoclave BUT NOT activated carbon) no similar losses due to “plating” are observed or reported. This can only be verified by undertaking pilot studies that go beyond this University-based research study.

5.2 CARBON-IN-AUTOCLAVE WITH HIGH CHLORIDE CONCENTRATION

All previous tests described in section 5.1 were carried out with low chloride ion concentrations namely 2.5 and 5 g/L with the latter yielding the best results-refer to Test 4 in Table 3). However, as reported significant gold deposition on the metallic surfaces of the 300 mL Ti autoclave was observed to occur despite the use of a glass liner and the removal of the internal metallic parts like stirring shaft and sampling tube as graphically shown in Figure 35. As shown gold deposition occured away from the solution in the liner due to apparent transfer of the chlorocomplexes with the evaporated water and reductive decomposition on the external metal surfaces.

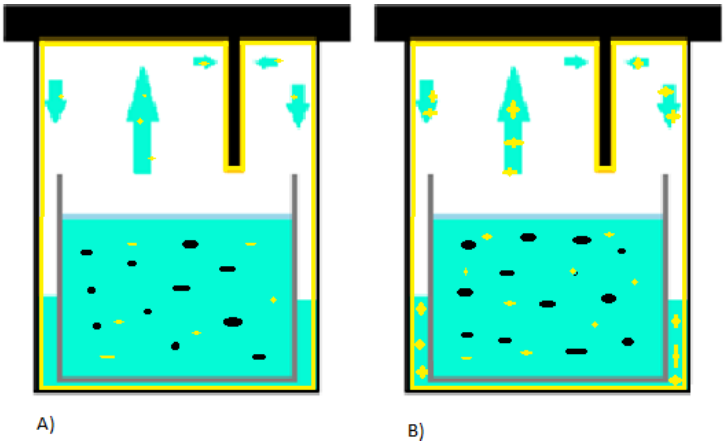
A) B)

Figure 35: Schematic of 300 mL Ti autoclave with liner depicting gold transfer-deposition on metal surfaces: A) Low chloride conc. case; B) High chloride ion conc. case

Considering that the stability of Au-chlorocomplexes increases with increasing chloride ion concentration-refer to Chapter 2 and the work of Blais [1], it was decided to perform carbon-in-autoclave experiments at higher [Cl] to verify (i) if this can reduce the extent of metal plating and (ii) if it would affect the adsorption of gold on carbon. The tests were run at the same conditions as Test 4 (Table 3), namely 53.3 g/L ground pyrite, 40 g/L activated carbon, 30 mg/L metallic gold, 10.2 g/L sodium, 10 atm oxygen pressure and 2 hours oxidation time. Tests were run at 155 ^{o}C and 200 ^{o}C. The results are shown in Figures 36 and 37. In both temperatures it is clearly seen the amount of gold reporting onto carbon to decrease significantly while the amount of gold plating on metallic surfaces increasing-refer to Figure 38.

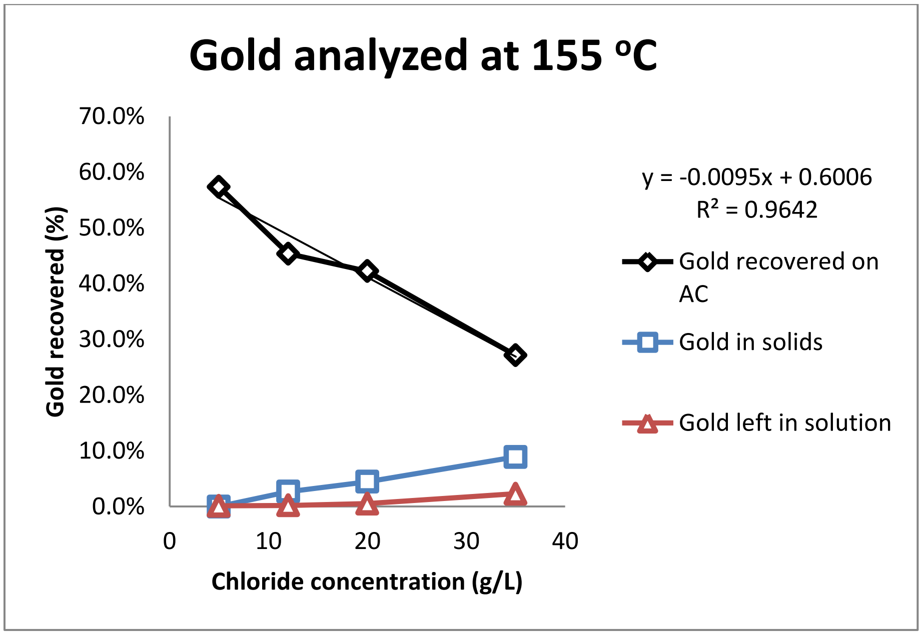

Figure 36: Percent gold reporting in the various phases at 155 ^{o}C as a function of chloride concentration

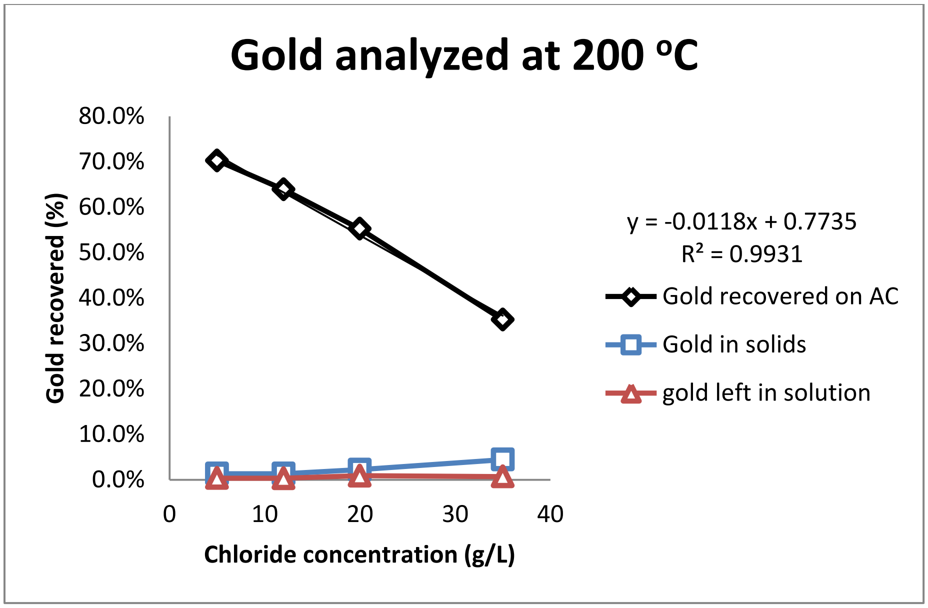

Figure 37: Percent gold reporting in the various phases at 200 °C as a function of chloride concentration

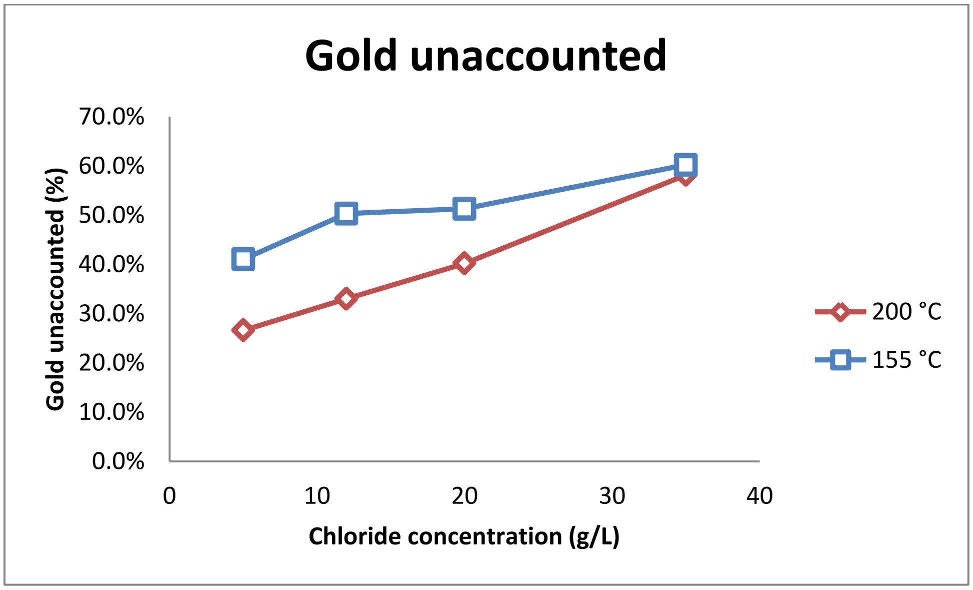

Figure 38: Percent gold plated at 155 and 200 °C as a function of chloride concentration

The reason for increased gold losses due to plating away from the solution in the liner suggests the higher the chloride ion concentration the higher the “escape” of gold out of the solution. This unreported behaviour of gold in a hydrometallurgical autoclave system may relate to similar gold chloride vapour phase stability behaviour reported in geochemistry [73]. It seems in this case that the increased stability conferred to the gold chloride complex at higher chloride concentration facilitated its transfer out of the solution and its deposition on the walls of the Ti vessel. The transfer of gold chloride into the vapour phase was confirmed by analyzing the water accumulated in the gap between the Pyrex liner and the Ti reactor interior wall, as seen in Figure 35. Typically approximately 40% of the water from the slurry would collect in this fashion during an experiment. This solution was always analyzed and was found to contain no gold in most tests. However when the chloride concentration was increased to 1M, it was found to contain approximately 5% of the gold, as illustrated in Figure 35 (B). The rest of the "unaccounted" gold had deposited on the metal surfaces. As for the apparent reduced amount of gold found on carbon this is not clear at the moment if it is the indirect effect of the increased loss of gold chlorocomplexes in the water vapour phase or if it reflects interference in gold chlorocomplex adsorption due to competition by the higher concentration chloride ions.

5.3 KINETICS AND PRODUCT CHARACTERIZATION

5.3.1 Gold recovery

In this series of experiments the effect of time on gold recovery by carbon adsorption in autoclave was studied at 155 and 200 ^{o}C. The employed conditions were the same with those of Test 4 in Table 3 above. In the case of the 155 ^{o}C test, due to its slower jarosite formation kinetics-refer to section 5.1, jarosite seed (6.67 g/L) was also added. However in contrast to the previous tests carried out in the 300 mL Ti autoclave equipped with a glass liner and using a magnetic Teflon stirrer, the 2L Ti Parr reactor was used fully equipped with internal titanium parts, in contact with the solution which was placed within a glass liner. This time the amount of gold plated was not simply assumed but was quantitatively determined by digesting overnight the internal titanium parts in a dilute solution of *aqua regia* and subsequent solution analysis by AAS; up to approximately 95 % mass balance was obtained.

A summary of the obtained results, in terms of gold deportment to different products, is given in Table 5.

Table 5: Percent gold distribution in products as function of time

TEMPERATURE	TIME (MIN)	% AU LEFT IN SOLUTION	% AU IN RESIDUE	% AU ON CARBON	% AU PLATED
155 °C	30	5.00	18.62	44.13	30.74
	60	4.00	12.44	53.78	28.28
	90	4.67	5.78	56.00	32.06
	120	3.33	3.11	58.67	33.39
200 °C	30	4.90	0.89	53.60	39.11
	60	4.40	4.00	54.67	35.43
	90	4.10	0.89	56.44	37.07
	120	3.47	0.89	53.60	39.11

As it can be seen this time the amount of gold recovered on carbon was lower than that of the previous series with the 300 mL autoclave having the liner but not agitator, this being due to higher amount of plated gold as a result of the larger metal surface.

The effect of time on gold deportment can be better evaluated by plotting the data as shown in Figures 39 and 40 for 155 °C and 200 °C respectively.

Tests at 155 °C: It is observed that for the experiments at 155 °C there was about 20% of gold remaining with the solids after 30 min progressively decreasing with the extension of time. XRD analysis of the 30 min residue (refer to the next characterization section) revealed the presence of unreacted pyrite. This means that the oxidation of pyrite (and possibly gold as well) was not complete. The data cannot differentiate between the kinetics of gold dissolution and pyrite oxidation or the possible interaction between the two due to galvanic coupling. It would appear however judging from the gold distribution curves of Figure 39 that gold dissolution parallels that of pyrite but further studies needed to substantiate the mechanism. Nevertheless the data reveal that the soluble gold reports onto carbon rather quickly as its level is essentially constant independent of reaction time. As the reaction proceeds, the gold recovered on carbon increased while the gold fraction in solids decreased eventually reaching ~60% recovery after 2 hours.

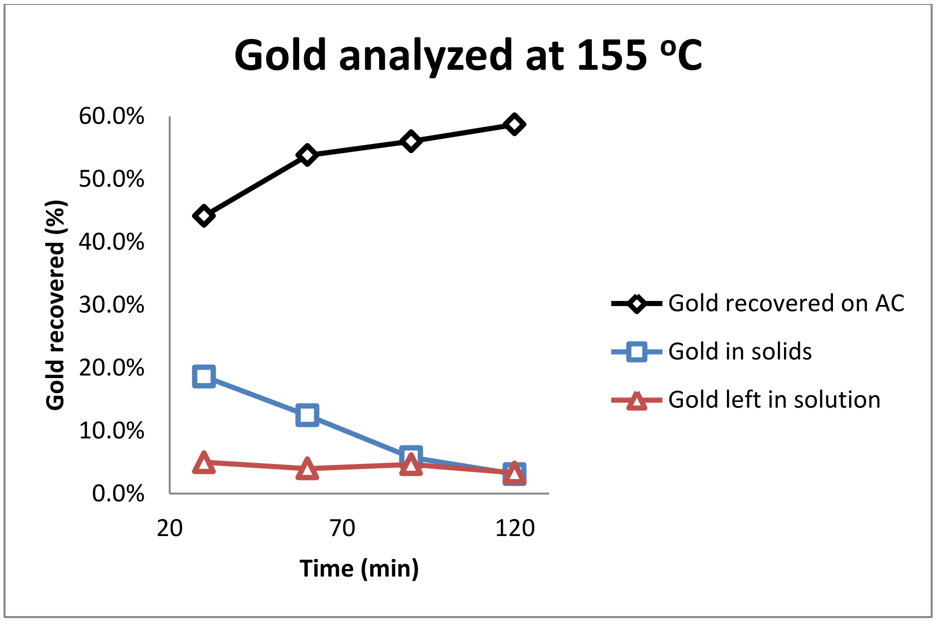

Figure 39: Percent gold reporting in the various phases as a function of time at 155 ^{o}C

The amount of gold plated on autoclave metal surfaces (as determined by digestion and analysis) was found to be independent of reaction time-refer to data of figure 40 below. This behaviour along with means to minimize its occurrence need to be studied further in future work.

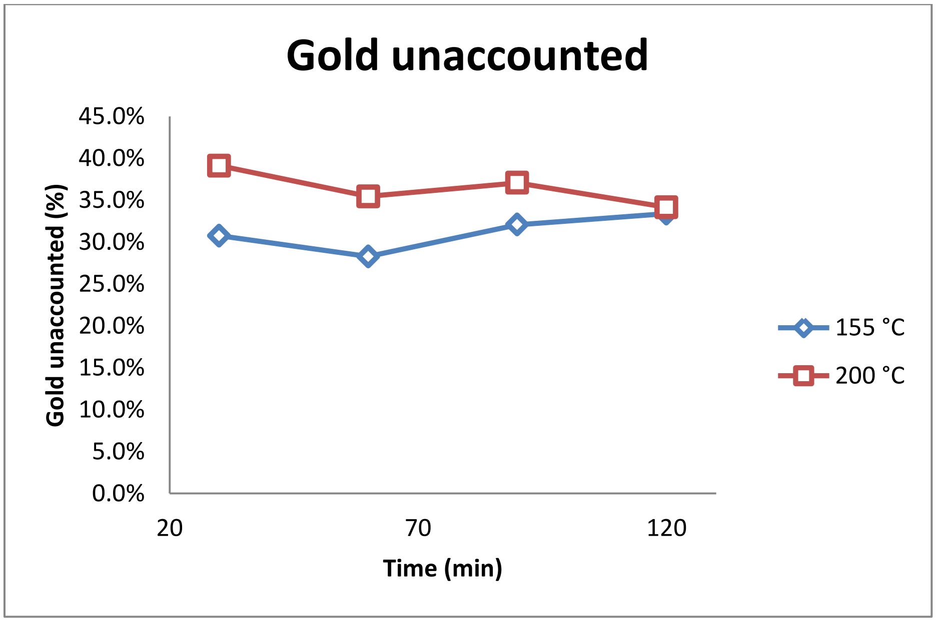

Figure 40: Percent gold plated on the reactor as function of time

Tests at 200 °C: For the time-dependent experiments performed at 200 °C, the reaction seems to be at completion after 30 minutes (Figure 41). The slight increase in recovery is correlated to a slight decrease in gold in solution consistent with the endothermic mechanism of gold uptake by carbon already mentioned earlier. Of interest here, in comparison to the 155 °C data, is that the amount of gold remaining with the residue is less than 1% in the case of 200 °C vs. 3% for 155 °C (Table 5). The origin of this difference is not clear. It can be due to different oxidation-dissolution kinetics or differences in the amount and speed of jarosite formation between the two temperatures. What is more critical is that the total amount of gold recovered on carbon was the same, i.e. ~ 60%, independent of the temperature at which the tests were run. This again reflects the plating problem that needs to be further studied.

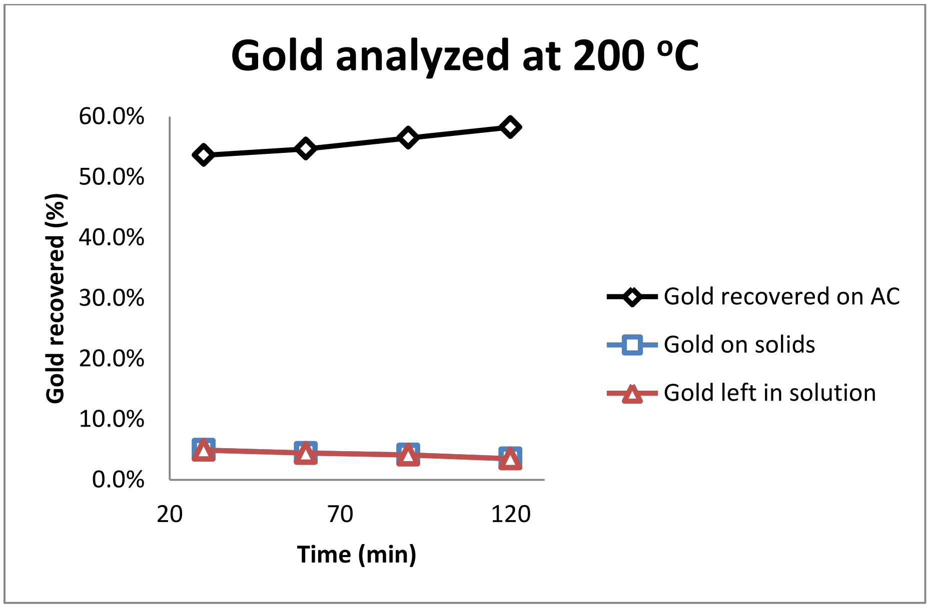

Figure 41: Percent gold reporting in the various phases as a function of time at 200 °C

5.3.2 Characterization of oxidation residue products

Upon XRD analysis all of the final (after 2 hours) pressure oxidized residues found to consist of natrojarosite. A typical XRD scan is shown in Figure 42 below. A comparison of this XRD pattern to that of reference natrojarosite material (00-030-1203) is provided in Figure 42. A good agreement between the two patterns exists although the residue contained as well some unaccounted peaks.

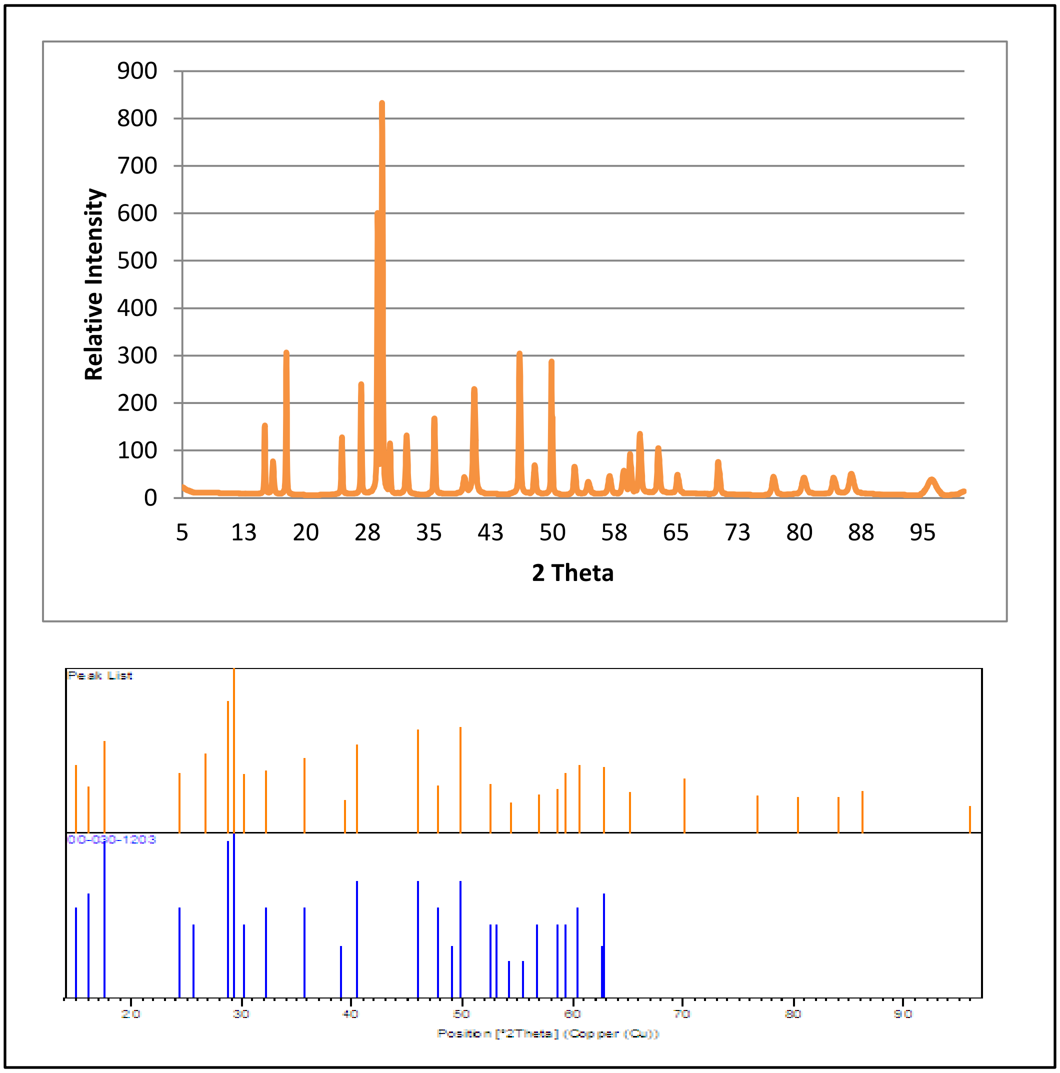

Figure 42: XRD spectra of oxidation residue product (200 ^oC, 2 h); below the oxidation product XRD pattern (yellow peaks) compared to the reference (00-030-1203) pattern of natrojarosite (blue peaks)

As mentioned in the 155 ^{o}C tests, after 30 min of oxidation the residue presented evidence of unreacted pyrite. This is illustrated with the XRD patterns of Figure 43.

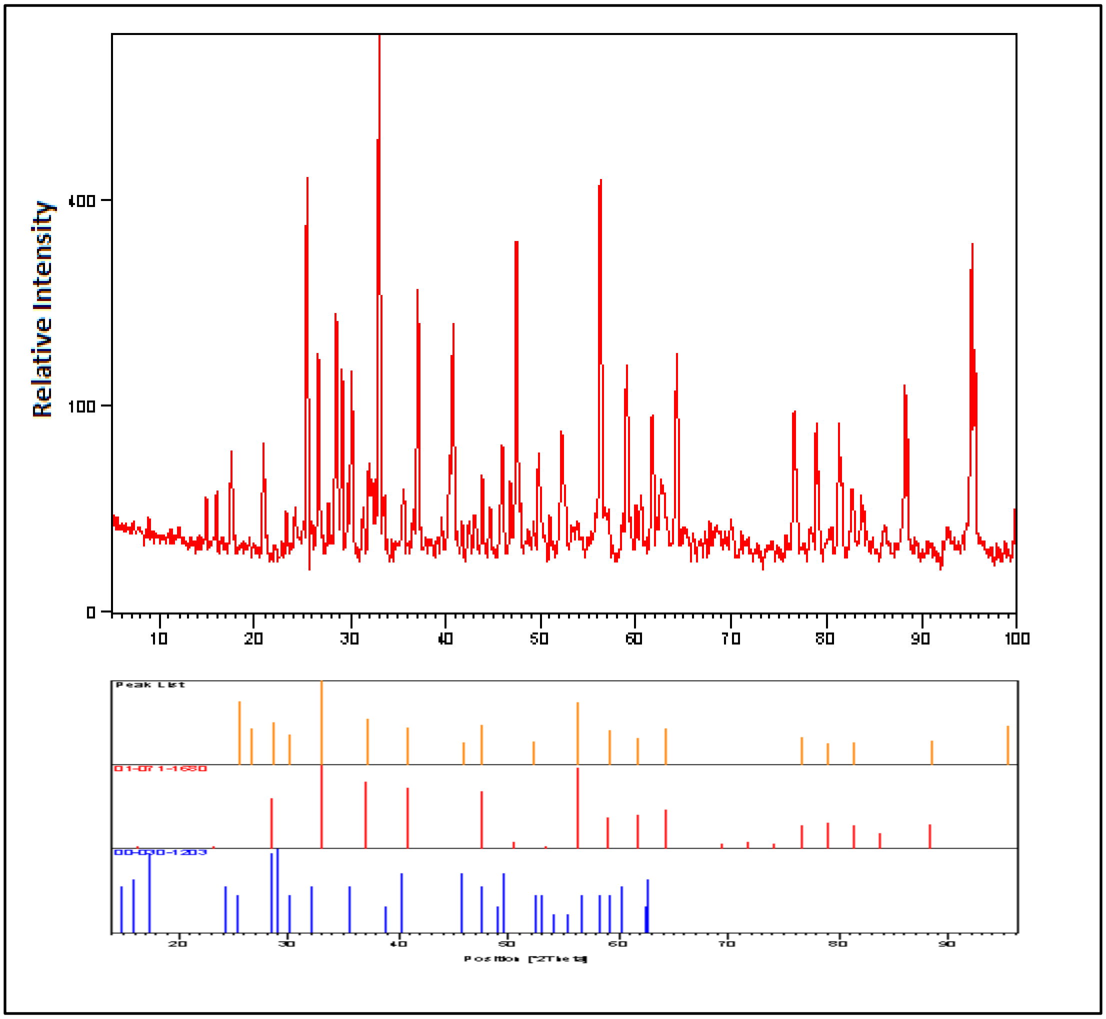

Figure 43: The XRD pattern (above) of the 155 ^{o}C oxidation residue obtained after 30 min; below the residue XRD pattern (orange) compared to reference patterns of pyrite (red) and natrojarosite (blue)

Finally, in Figure 44, a typical SEM image of jarosite residue is shown. Due to its trace amount residual gold is not visible.

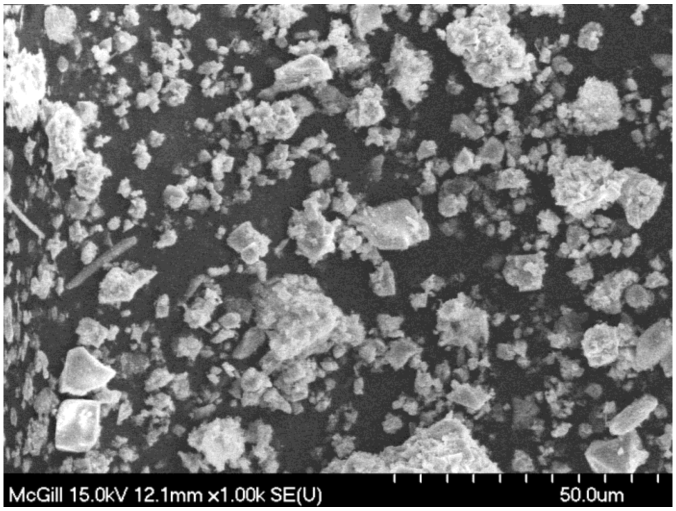

Figure 44: SEM of jarosite residue (200 ^{o}C, 2 h)

5.3.3 Characterization of gold loaded-activated carbon

Two gold loaded-activated carbon samples were analysed by SEM and EDS. The first sample was the product of a 200 ^{o}C pressure oxidation test (2 hours) performed in the 2L Parr titanium autoclave (see section 5.2.3). The second one was obtained from a 155 ^{o}C test (2 hours) performed in the 300 mL Parr titanium autoclave (see section 5.1). The SEM/EDS images/scans are shown in Figures 45 and 46 respectively. On both samples, one site was chosen for EDS analysis that revealed the presence of gold clusters confirming the reduction of gold (at least in part) to metallic state. Although the formation of metallic gold could have had happened during the stage of sample preparation prior (drying) and during SEM observation, at this point combined with the findings of XPS analysis (reported in Chapter 4) and further described later, it is postulated that its formation occurred at least in part during the adsorption stage. Comparison between the two samples indicates the sample obtained from the 155 ^{o}C experiment to contain a chloride signal not evident in the 200 ^{o}C sample. This may indicate that there are differences in the mechanism of uptake with some of the gold present as chlorocomplex (Au(I)) at 155 ^{o}C but not at 200 ^{o}C. This elemental discrepancy when analyzing the gold clusters, which had formed during pressure oxidation, is investigated further in a subsequent section using XPS.

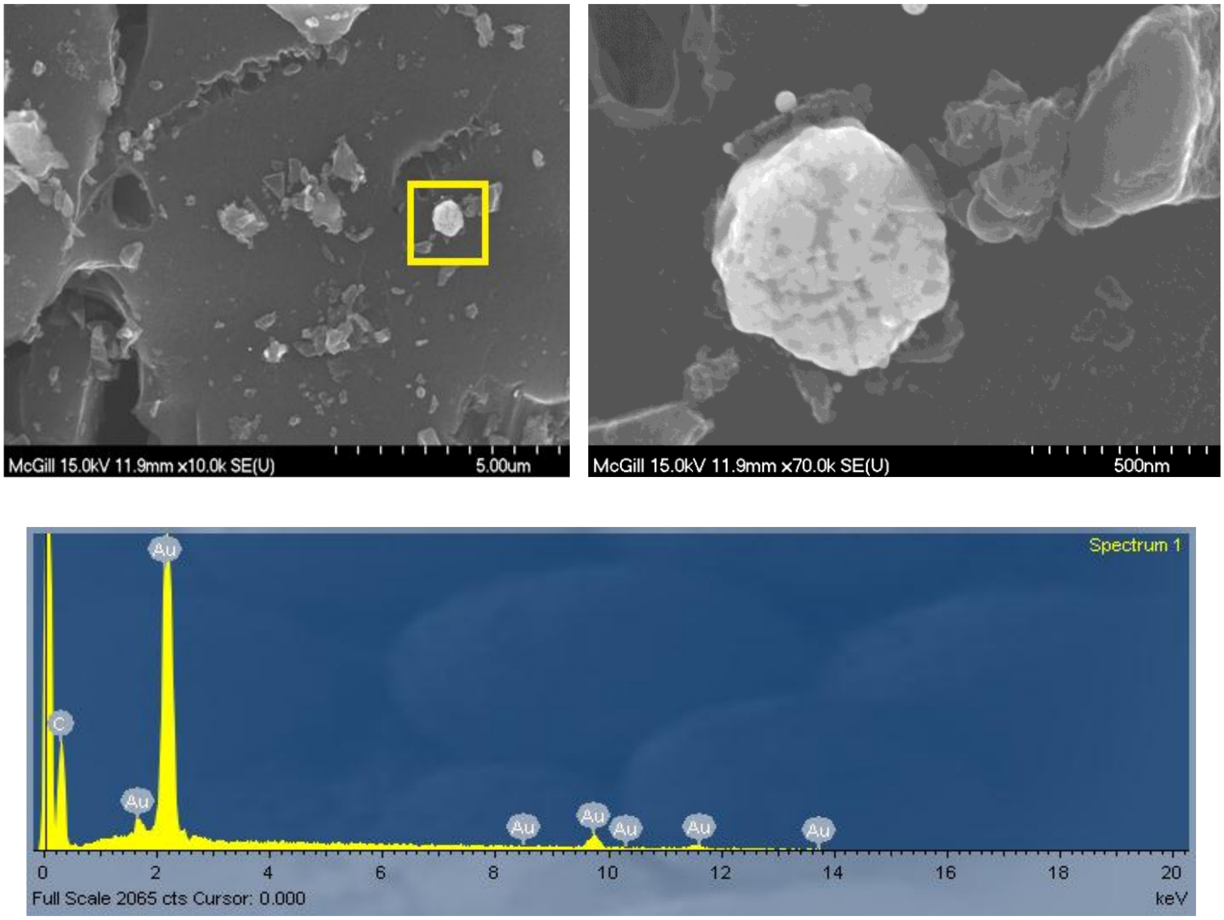

Figure 45: SEM image (above) and EDS spectrum (below) of gold loaded activated carbon obtained from a 200 °C test

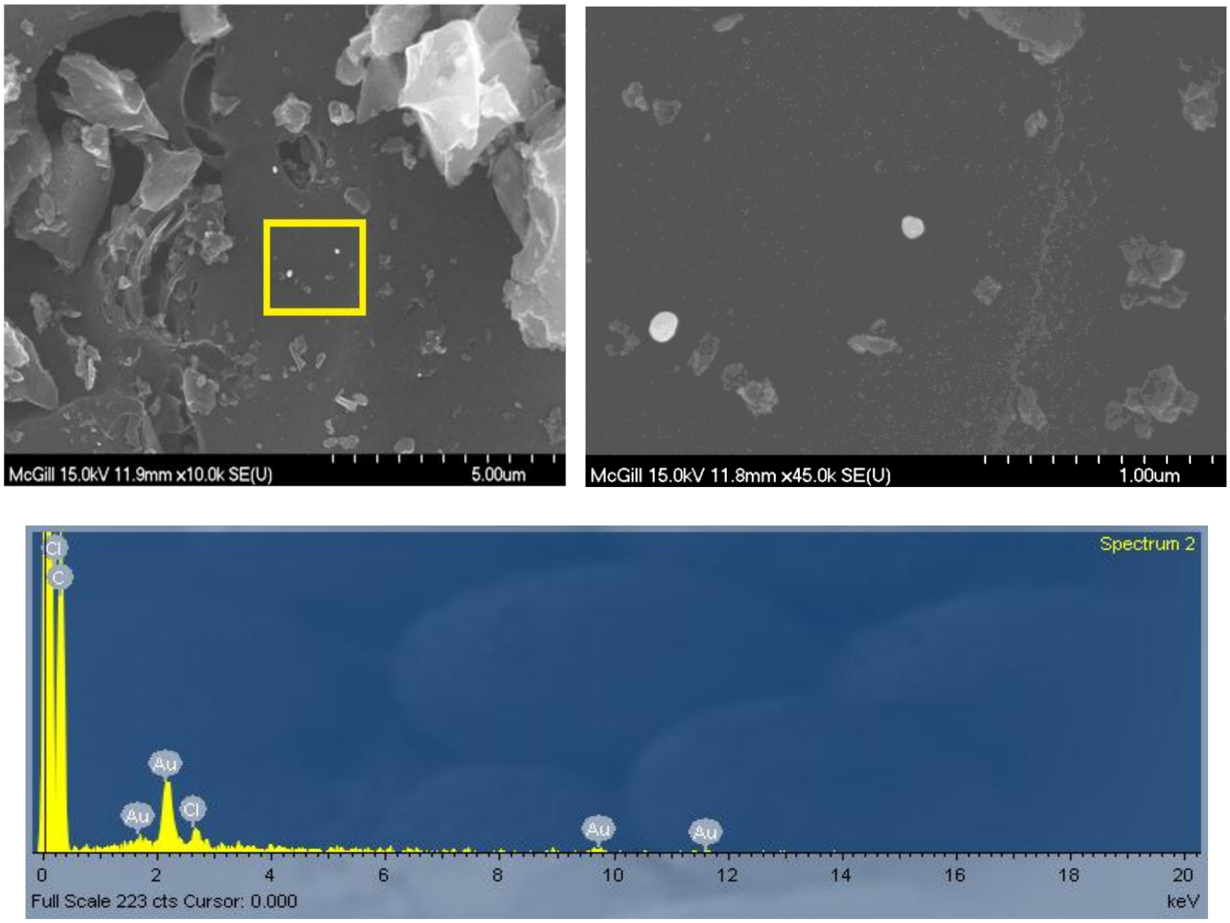

Figure 46: SEM image (above) and EDS spectrum (below) of gold loaded activated carbon obtained from a 155 ^{o}C test

5.3.4 XPS of gold loaded activated carbon at 200 ^{o}C

As reported in section 4.2 gold loaded on activated carbon was found to be in two forms, metallic gold and Au(I)Cl. Here XPS is used to verify if the nature of loaded gold on carbon remains the same under pressure leaching at 200 ºC. The relevant XPS spectra are shown in Figures 47 and 48. As we can observe from the spectra of the gold at low and high concentrations, the appearance of the AuCl species has significantly diminished in comparison to that at 25 or 95 ºC (spectra presented in section 4.2). These observations are further proved quantitatively from the de-convolution analysis performed (Table 1 in section 4.2). According to this data, ~ 70% of gold is present in metallic form and the rest as Au(I)Cl as opposed to ~ 65% and ~ 50% of metallic gold at 95 and 20 ºC respectively.

The higher occurrence of metallic gold at higher temperature can be explained on the basis of thermodynamics favouring the destabilization of the chlorocomplex and the reduction of gold to metallic state. It is still interesting nevertheless that even at 200 ºC some gold chlorocomplex persists; i.e. not complete reduction to metallic state occurs, a behaviour that points to kinetic resistance, the study of which is beyond the scope of this project.

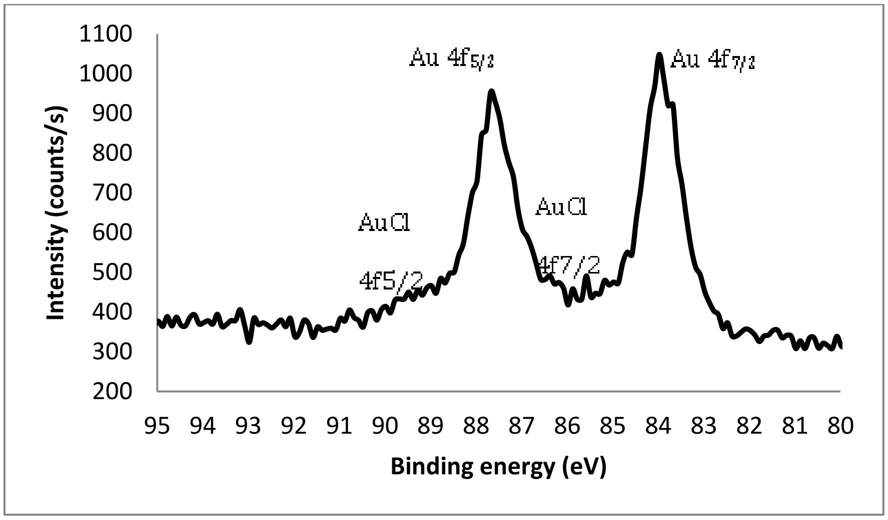

Figure 47: XPS spectra of gold loaded on activated carbon at 200 ^{o}C with low chloride concentration (0.05M)

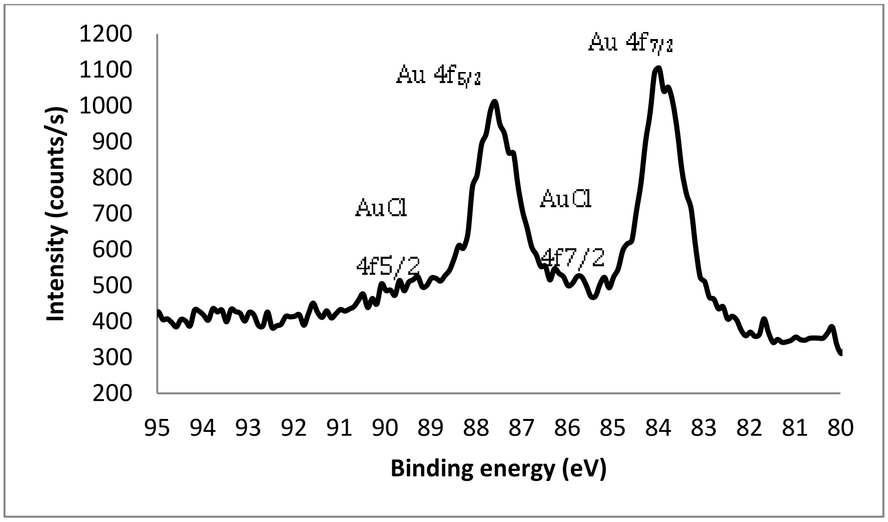

Figure 48: XPS spectra of gold loaded on activated carbon at 200 ^{o}C with a high chloride concentration (1M)

5.4 CARBON-IN-AUTOCLAVE TESTING USING A GLASS PRESSURE REACTOR AND A REAL CONCENTRATE

After the Ti autoclave experiments yielded results where some of the gold found to deposit/plate on metal surfaces, it was decided to fully test the carbon-in autoclave concept by employing a glass autoclave with no metal parts. Because of the limited pressure rating of the glass autoclave, tests were run only at 155 ℃. There were three tests, two employing the standard synthetic pyrite/gold feed (as in Test 4 of Table 3) while the third test involved pressure leaching of a copper/gold concentrate supplied by Teck's CESL group ("Santa-Maria concentrate")[3]. The concentration of pyrite (or concentrate) used in this series of tests was half (26.65 g/L) of that used in the previous series of tests (53.3 g/L), while the reaction time was longer than 2 hours used in the previous tests. This was deemed necessary due to lower partial oxygen pressure allowed with the glass autoclave and the inevitable associated slower kinetics. The obtained gold recovery results are summarized in Table 6 and plotted in Figure 49. This time gold recovery on carbon exceeded 95% proving the capability of activated carbon to capture gold quantitatively in the autoclave under pressure leaching conditions.

Table 6: Glass autoclave test results (experimental conditions: 30 mg/L gold in Tests 1 and 2 and 0.6 mg/L in Teck test; reaction time=3 hrs; 155 °C)

TEST ID-FIG 49	PYRITE (G/L)	A.C. (G/L)	PO_2 (ATM)	TIME (HRS	CL (G/L)	NA (G/L)	%AU IN SOLUTION	% AU SOLIDS	%AU IN CARBON
1	26.65	40	3	3	5	10.2	1.07%	23.33%	75.60%
2	26.65	40	4	4	5	10.2	0.87%	0.00%	97.87%
Teck Santa Maria conc	26.65	40	4	4	5	6.67	4.90%	0.00%	95.86%

---

[3] Santa Maria concentrate analysis: 35 % liberated gold, 38 % gold occurring in non-copper sulphides, 17 % gold occurring in various bismuth minerals, 9% gold occurred in copper sulphides, and the remaining 1% was locked within silicates, 22.9 ppm gold content overall which is distributed as 84% electrum, 13 % native gold and 3% as sylvanite $(Au,Ag)_2Te_4$.

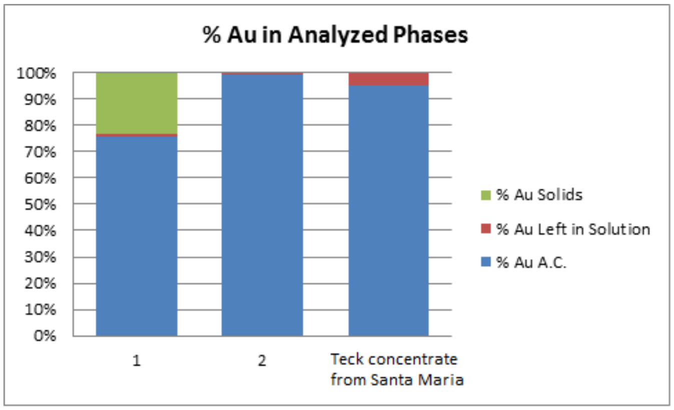

Figure 49: Percent gold distribution in glass autoclave tests at 155 °C

In Test 1, there was a significant fraction (~25%) of gold found in the solids. This was thought to be due to incomplete reaction as evident by the presence (Figure A1 in the Appendix) of unreacted pyrite in the final solid product. To push the reaction to completion, Test 2 was run for 4 hours in total and the partial oxygen pressure was set at 4 atm, which borders on the glass autoclave's upper limit. A longer time was needed because the oxidation was apparently very slow due to the lack of dissolved ferrous/ferric and once the cycle of oxidation began, the product formed readily as natrojarosite (Figure A2 in the Appendix). This time a record 97% gold recovery on carbon was achieved. This experiment affirms the possibility of simultaneous pressure leaching and adsorption on activated carbon within the autoclave.

Having successfully demonstrated that quantitative in-situ gold adsorption is in principle feasible with a synthetic feed, a next confirmatory test was run using a gold carrying (22.9 ppm gold content) concentrate sample provided by Teck (Santa Maria). Once more, very high gold recovery via loading on carbon was obtained in the vicinity of 95%. This time the balance of gold was detected to be in solution (~5%) but this may be due to analytical error (AA used in solution analysis) as the gold concentration was very low (estimated at 0.6 mg/L assuming 100% of gold from the concentrate (22.9 ppm) having dissolved). However, the gold content of the carbon is considered valid as in this case Neutron Activation was employed, which is known for its high (ppb range) sensitivity.

5.5 CONCEPTUAL FLOW SHEETS INCORPORATING THE CARBON-IN-AUTOCLAVE CONCEPT

Although it is premature to talk of a process as such, before larger scale tests are run and the issue of gold plating as well as the assessment of carbon resistance to attrition when passed through an autoclave circuit are addressed satisfactorily, it is informative to consider the integration of the new CIA ("carbon-in-autoclave") concept into POX or PL flow sheets. First, the case of refractory gold processing is addressed as shown in Figure 50 comparing to the conventional one, Figure 19, helps to identify the potentially great process, environmental, and economic advantages the carbon-in-autoclave scheme can bring if it proves feasible. Among these advantages are: (i) process simplification via the elimination of several process steps; (ii) the elimination of these steps translates to capital (less equipment required) and operating (no cyanide and associated chemicals for its destruction and neutralization required); and (iii) environmental acceptance due to cyanide elimination. The presented flow sheet of Figure 50 indicates partial recycling of treated effluent that can provide a source of sodium and chloride (in addition to water of course) thus reducing the purchase of sodium salts. In addition, a fraction of the tails may be recycled (as needed) to act as jarosite seed.

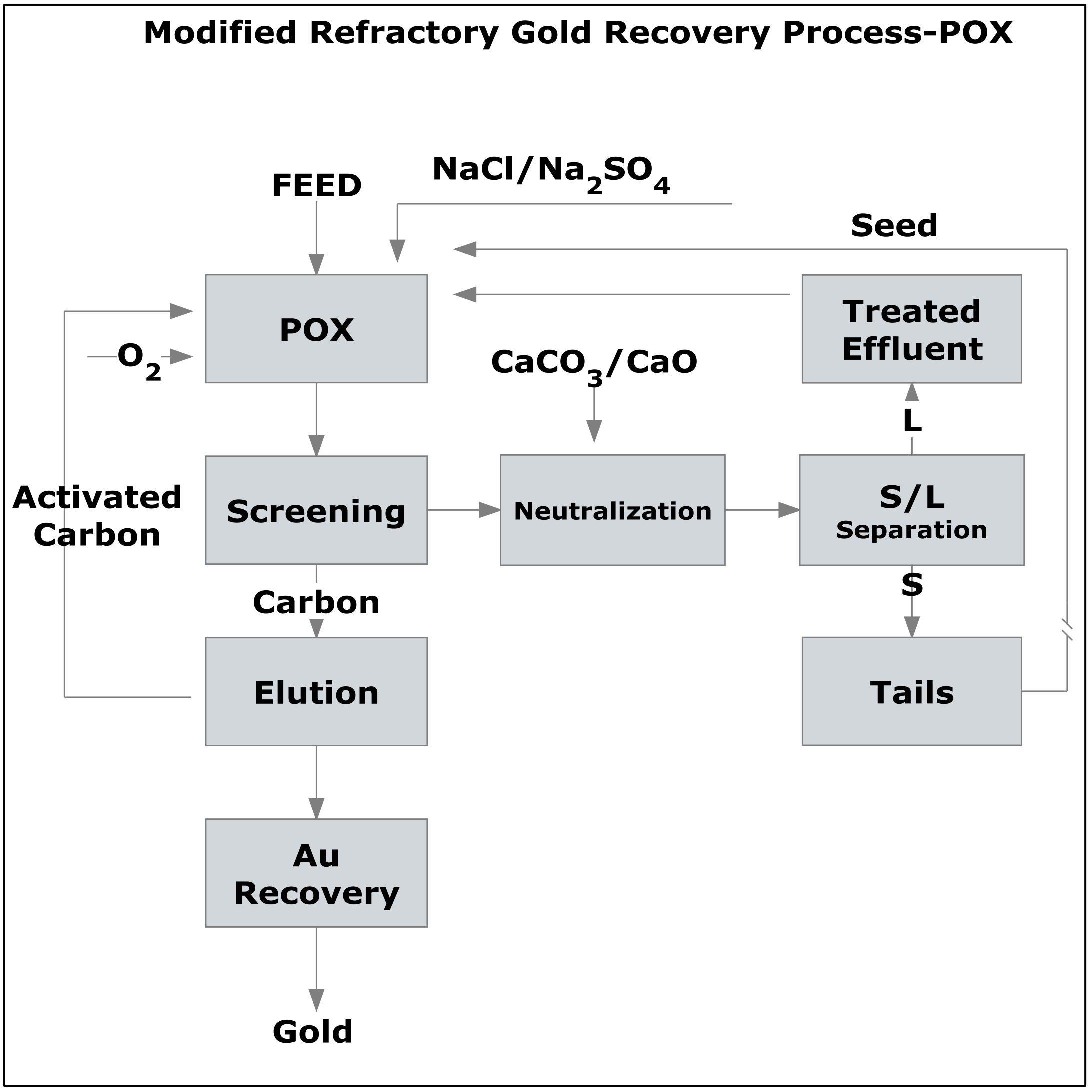

Figure 50: Conceptual gold recovery flowsheet ("Carbon-in Autoclave" concept; CIA) for a refractory gold feedstock

Application of the new "carbon-in-autoclave" (CIA) concept to copper pressure leaching, in particular the CESL process, is shown with the aid of the flow sheet of Figure 51. Chloride is already added in the CESL autoclave so the new CIA concept is ideally suited to apply to this process. However, at present any gold chlorocomplexes that may have formed during pressure leaching (this issue has not been discussed in the hydrometallurgical literature) decompose (presumably) into metallic gold reporting with the residue. This interpretation is consistent with thermodynamic and experimental tests performed in our laboratory by Blais [1]. Again as in Figure 50 (POX application), sodium sulphate and activated carbon are added/recycled in the autoclave along part of the produced tails to act as seed. Actually such seed recycling to promote jarosite precipitation may not be necessary since in a continuous reactor the solids in the autoclave can behave as seeding material.

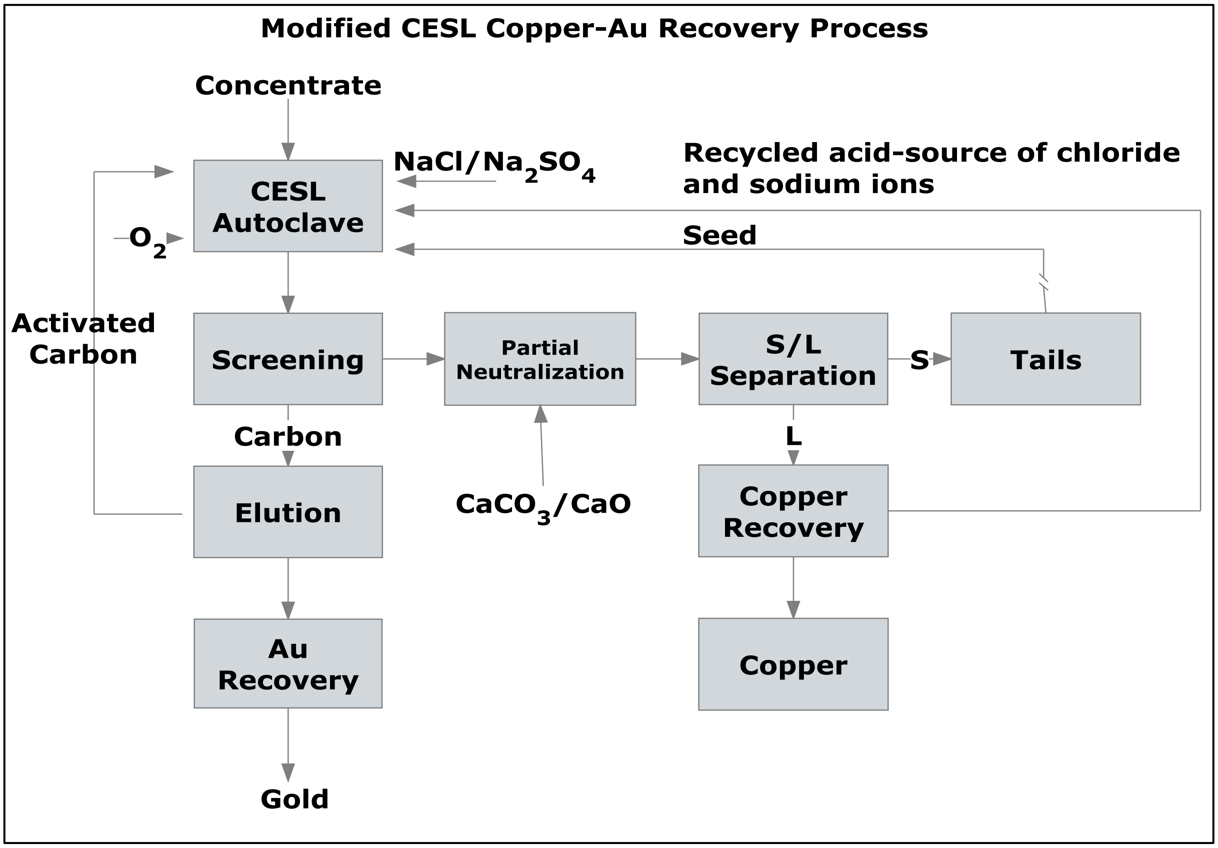

Figure 51: Conceptual CESL-type copper pressure leaching process flowsheet making use of the Carbon-in-Autoclave (CIA) concept

Chapter 6. CONCLUSIONS

In this thesis, the behaviour of gold (III) chloride was investigated in an acidic environment in order to evaluate the possibility of gold adsorbing on activated carbon under pressure oxidation-leaching conditions. First, the adsorption of gold(III) chloride on activated carbon was studied as a function of temperature (20-95 ºC) in order to determine its kinetics and understand the associated mechanism before embarking into the more complex autoclave leaching system. The initial gold(III) chloride adsorption at 20, 60 and 95 ^{o}C, yielded increasing adsorption profiles with increasing temperature. This was very encouraging for high temperature adsorption and an activation energy of 8.69 kJ/mol was determined. This value clearly points towards a diffusion-controlled process. XPS spectra of gold-loaded carbon samples obtained with a low (0.05M) and high chloride (1M) concentration at 20 and 95 ^{o}C revealed the presence of gold in part as Au(I)Cl and in part as metallic gold. It was observed that the amount of Au(I) decreased with increasing temperature and increased with increasing chloride ion concentration, in consistence with the relative stability of the Au(I)-chlorocomplex.

Based on the information gathered, it is postulated that soluble gold(III)-chloro complex upon initial adsorption on carbon are reduced to intermediate gold(I)Cl complex with part of the latter further reduced to metallic Au.

Following the atmospheric pressure adsorption tests, carbon-in-autoclave (CIA) tests were carried out involving pressure oxidation of pyrite at 155 and 200 ^{o}C in order to evaluate/determine the deportment of gold at varying conditions. Two initial observations were made with these experiments, firstly that the oxidation product hematite results in a “preg-robbing” effect due to gold chloride adsorption and secondly that not all of the gold could be accounted for due to apparent deposition on metallic surfaces. Subsequent to these observations, CIA pressure oxidation of pyrite at different times and chloride concentrations was carried out. According to this series of tests, at 200 ^{o}C, the oxidation was complete after 30 minutes and all gold (except the amount deposited on the metal surfaces) had adsorbed on the activated carbon within the same time of 30 minutes. This implies that as soon as gold mobilized as a chlorocomplex via oxidation and complexation, it adsorbed on carbon which is a behaviour consistent with the observed diffusion-controlled adsorption kinetics. On the other hand, at 155 ^{o}C, the kinetics were slower. Thus there was about 20% of gold remaining with the solids after 30 min progressively decreasing with the extension of time down to ~5% after 90 min. XRD analysis of the 30 min residue revealed the presence of unreacted pyrite. This means that the oxidation of pyrite (and possibly gold as well) was not complete. The data could not differentiate between the kinetics of gold dissolution and pyrite oxidation, however, the available evidence suggested that gold dissolution paralleled that of pyrite. It is further conceivable that gold dissolution cannot proceed to completion unless first pyrite is fully oxidized due to galvanic coupling. As soon as gold is solubilized, it appears to quickly adsorb onto the activated carbon.

Tests run at increasing chloride ion concentrations (from 5 to 35 g/L) revealed to register lower gold recovery on carbon due to increasing gold plating on metal surfaces outside the glass liner of the Ti autoclave. There appears that with higher chloride ion concentration there was higher tendency for “escape” of gold out of the solution. It seems in this case that the increased stability conferred to the gold chloride complex at higher chloride concentration facilitated its transfer out of the solution and its deposition on the walls of the Ti vessel. In order to prove finally the validity of the carbon-in-autoclave concept without the undesirable occurrence of gold plating, pressure oxidation experiments in a low pressure glass autoclave were attempted at 155 ºC. Due to the lower pressure of oxygen applied (4 atm vs. 10 atm for the Ti autoclave), the kinetics were much slower hence the reactions were allowed to proceed for longer time (3-4 hours) to obtain total oxidation of pyrite. These low pressure oxidation experiments yielded recoveries above 95% (compared to the best titanium recoveries of approximately 75%) for both pyrite/gold synthetic feed as well as a real copper/gold concentrate.

It is obvious that more work is needed to investigate the full technical feasibility of the CIA concept by paying particular attention to the elimination of the plating problem, the ability of carbon to resist fragmentation in strongly agitated and oxygenated slurry environment, as well as the effect of various impurities.

REFERENCES

1) Blais, D., 2010, "Behavior of Gold(III) Chloride During the Precipitation of Iron (III)/Arsenic(V) in Aqueous Media Under Atmospheric and Pressure Conditions", M.Eng. Thesis, McGill University.
2) Marsden, J. O. and House, C. L., 2006, "The Chemistry of Gold Extraction", 2nd Ed, Ellis Horwood, New York, NY.
3) Laplante, A. R. and Staunton, W., 2003, "The Link Between Gravity Recovery and Hydrometallurgy: The Case for Gold", Proceedings of Hydrometallurgy 2003- Fifth Conference in Honour of Professor Ian Ritchie- Volume 1: Leaching and Solution Purification, Young, C., Alfantazi, A. Anderson, C., James, A., Dresinger and Harris, B., TMS, Warrendale, PA, pp.65-74.
4) Marsden, J. O., 2006, "Overview of Gold Processing Techniques around the World", Mineral and Metallurgical Processing, Vol 23, no. 3, pp. 121-125.
5) Miller, G. C. and Pritsos, C. A., 2001, "Unresolved Problems with the Use of Cyanide in Open Pit Precious Metal Mining", in proceedings of Cyanide: Social, Industrial and Economic Aspects, TMS, Warrendale, PA, pp. 73-81.
6) Mudler, T. and Smith, A., 1991, "The Chemistry and Treatment of Cyanide Wastes", Mining Journal Books, London, England.
7) Young, C. A., 2001, "Cyanide: Social, Industrial and Economic Aspects", TMS, Warrendale, PA.
8) Senanayake, G., 2004, "Gold Leaching in Non-cyanide Lixiviant Systems: Critical Issues on Fundamentals and Applications", Mineral Engineering, Vol. 17, pp. 785-801.
9) G. J. Sparrow and J.T. Woodcock, 1995, "Cyanide and Other Lixiviant Leaching Systems for Gold with Some Practical Applications", Mineral Processing and Extractive Metallurgy Review, 14:3-4, pp. 193-247.
10) Haque. K. E., 1987, "Gold Leaching from Refractory Ores-Literature Review", Mineral Processing and Extractive Metallurgy Review, Vol. 26, pp. 235-254.
11) Demopoulos, G.P. and Papangelakis, V. G.,l989, "Recent Advances in Refractory Gold Processing", CIM Bulletin, 82(931), pp. 85-91.
12) Demopoulos, G.P. and Papangelakis, V. G., 1990, "Acid Pressure Oxidation of Arsenopyrite: Part 1, Reaction Chemistry", Canadian Metallurgical Quarterly, Vol. 29, pp. 1-12.
13) Demopoulos, G.P. and Papangelakis, V. G., 1990, "Acid Pressure Oxidation of Arsenopyrite: Part 2, Reaction Kinetics", Canadian Metallurgical Quarterly, Vol. 29, pp. 13-20.
14) Papangelakis, V. G., Demopoulos, G.P., 1991, "Acid Pressure Oxidation of Pyrite: Reaction Kinetics", Hydrometallurgy, Vol. 26, pp. 309-325
15) Cheng, T. and Demopoulos, G.P, 2004, "Hydrolysis of Ferric Sulfate in the Presence of Zinc Sulfate at 200 °C: Precipitation Kinetics and Product Characterization", Ind. Eng. Chem. Res., Vol. 43(20): p. 6299–6308.
16) Das, G. K., Acharya, S., and, S., Das, R. P., 1996, "Jarosite: A Review", Mineral Processing Extractive Metallurgy Review, Vol. 16, pp. 185-210.

17) Gomez, M. A., Becze, L., Cutler, J. N. and Demopoulos, G.P., 2011, “Hydrothermal Reaction Chemistry and Characterization of Ferric Arsenate Phases Precipitated from $Fe_2(SO_4)_3$-As_2O_5-H_2SO_4 Solutions”, Hydrometallurgy, Vol.107, pp. 74–90.
18) Defreyne, J., Grieve, W., Jones, D. L., Mayhew, K., 2006,“The Role of Iron in the CESL Process”, In Iron Control Technologies; Dutrizac, J. E., Riveros, P. A., Eds.; CIM, Montreal, pp. 205-221.
19) Gomez, M. A., Becze, L., Ceklin, M. and Demopoulos, G. P., 2011, “The Effect of Copper on the Formation of Scorodite ($FeAsO_4 \cdot 2H_2O$) Under Hydrothermal Conditions: Evidence for a hydrated ferric cupric arsenate sulfate short-lived intermediate”, J. Colloid and Interface Sci. Vol. 360, pp. 508–518
20) Marsden, J. O. and Wilmot, J. C., 2007, “Sulfate-Based Process Flowsheet Option for Hydrometallurgical Treatment of Copper Sulfide Concentrates”, in Proceedings, The John E. Dutrizac International Symposium on Copper Hydrometallurgy, Vol IV, Book 1, Riveros, P. A., Dixon, D. G., Dreisinger, D. B., Collins, M. J., CIM, Montreal, QC, Book 1, pp. 77-100.
21) Keith Mayhew, Pardeep Parhar, Henry Salomon-de-Friedberg, “CESL Process as Applied to Enargite-Rich Copper Concentrates”, Proceedings of Copper 2010 Conference, Hamburg, DE, June 2010.
22) Defreyne J. and Ole Wagner,“Unlocking Value in Copper Arsenic Sulphide Ressources with the Copper-Arsenic CESL Technology“, presented at HydroCopper 2011, held in Vina del Mar, Chile, July 2011.
23) Barr G., Willy Grieve, David Jones, and Keith Mayhew, 2007, “The New CESL Gold Process”, presented at ALTA 2007 (accessed through www.cesl.com).
24) Fraser, K. S., Wells, J. A., 1991, “Processing of Refractory Gold Ores”, Minerals Engineering, Vol. 4, pp. 1029-1041.
25) Rees, K. L. and Deventer, J. S. J., 2000, “Preg-Robbing Phenomena in the Cyanidation of Sulphide Gold Ores”, Hydrometallurgy, Vol. 58, pp. 61-88.
26) Adams, M. D., Burger, A. M., 1998, “Characterization and Blinding of Carbonaceous Preg-Robbers in Gold Ores”, Minerals Engineering, Vol. 11, No. 10, pp. 919-927.
27) Kovalev, K.R., Kalinin, Yu. A., Naumov, E.A., Kolesnikova, M.K. and Korolyuk, V.N., 2011, “Gold-Bearing Arsenopyrite in Eastern Kazakhstan Gold Sulphide Deposits”, Russian Geology and Geophysics, Vol. 52, pp. 178-192.
28) Helm, M., Vaughan, J., Staunton, W.P. and Avraamides, J., 2009, “An Investigation of the Carbonaceous components of Preg-Robbing Gold Ores” World Gold Conference 2009, The Southern African Institute of Mining and Metallurgy, pp. 139-122.
29) Bailey, L. K., Peters, E., 1976, “Decomposition of Pyrite in Acids by Pressure Leaching and Anodization: The Case for an Electrochemical Mechanism”, Canadian Metallurgical Quarterly, Vol. 15, pp. 333-344.
30) Rimstidt, D. J., Vaughan, D. J., 2002, “Pyrite Oxidation: A State of the Art Assessment of the Reaction Mechanism” Geochimica et Cosmochimica Acta, Vol. 67, No. 5, pp. 873-880.
31) Long, H., Dixon, D. G., 2003, “Pressure Oxidation of Pyrite in Sulphuric Acid Media: a Kinetic Study”, Hydrometallurgy, Vol. 73, pp. 335-349.

32) G.P. Demopoulos and V.G. Papangelakis, 1987, "Acid Pressure Oxidation of Refractory Gold Mineral Carriers", Int'l Symp. on Gold Metallurgy, R.S. Salter et al. (Eds.), CIM, Montreal, Que., pp. 341-357.
33) King, W. E. and Lewis, J. A., 1980, “Simultaneous Effect of Oxygen and Ferric Iron on Pyrite Oxidation in an Aqueous Media”, Industrial and Engineering Chemistry Process Design and Development”, Vol. 19 No. 4, pp. 719-722.
34) Zheng, C. Q., Allen, C. C., Bautista, R. G., 1986, “Kinetic Study of the Oxidation of Pyrite in Aqueous Ferric Sulphate Media”, Industrial and Engineering Chemistry Process Design and Development”, Vol. 25, No. 1, pp.308-317.
35) Holmes, P. R. and Crundwell, F. K., 2000, “The Kinetics of the Oxidation of Pyrite by Ferric Ions and Dissolved Oxygen: an Electrochemical Study”, Geochemica et Cosmochimica Acta, vol. 64, No. 2, pp. 263-274.
36) Littlejohn, P. O. L., 2008, “The Enhancing Effect of Pyrite on the Kinetics of Ferrous Iron Oxidation by Dissolved Oxygen”, M.Sc. Thesis, The University of British Columbia.
37)Urbano, G., Reyes, V. E., Veloz, M. A., Gonzalez, I. And Cruz, J., 2008, “Pyrite and Arsenopyrite Galvanic Interaction and Electrochemical Reactivity”, Journal of Physical Chemistry, Vol. 112, pp. 10453-10461.
38) Lowson, R. T., 1982, “Aqueous Oxidation of Pyrite by Molecular Oxygen”, Chemical Reviews, vol. 82, No. 5, pp. 461-493.
39) Corkhill, C. L. and Vaughan, D. J., 2009, “Arsenopyrite Oxidation: A Review”, Applied Geochemistry, Vol. 24, pp. 2342-2361.
40)Lotens, J. P., Wesker, E., 1987, “The Behaviour of Sulphur in the Oxidative Leaching of Sulphidic Minerals”, Hydrometallurgy, Vol. 18, pp. 39-54.
41) Biernat, R. J. and Robins R. G., 1972, “High Temperature Potential/pH Diagrams for the Iron-Water and the Iron-Water-Sulfur Systems”, Electrochimica Acta, Vol. 17, pp. 1261-1283.
42)Dutrizac, J. E., 1991, “The Precipitation of Lead Jarosite from Chloride Rich Media”, Hydrometallurgy, Vol. 26, pp. 327-346.
43) Dutrizac, J. E., 1995, “The Effect of Seeding on the Rate of Precipitation of Ammonium Jarosite and Sodium Jarosite”, Hydrometallurgy, Vol. 42, pp.293-312.
44) Dutrizac, J. E. and Kaiman, S., 1976, “Synthesis and Properties of Jarosite-type compounds”, Canadian Mineralogist, Vol. 14, pp. 151-158.
45) Ketcham, V. J., O’Reilly, J. F., Vardill, W. D., 1993, “The Lihir Gold Project: Process Plant Design”, Minerals Engineering, Vol. 6, No. 8-10, pp. 1037-1065.
46) Garofalo, D., 2009, AEM Today: Agnico-Eagle Mines-Limited 2009 Annual Report, Agnico Eagle Mines: Toronto, Canada.
47) G.P. Demopoulos, V.G. Papangelakis, B. Buchanan and P.R. Mainwaring, l989, "Direct Solubilization of Refractory Gold by Pressure Chloride Leaching", Extraction Metallurgy '89, IMM, London, UK, pp. 603-627.
48) Liu, J. Q. and Nicol, M. J., 2002, “Thermodynamic and Kinetics of the Dissolution of Gold Under Pressure Oxidation Conditions in the Presence of Chloride”, Canadian Metallurgy Quarterly, vol. 41, pp. 409-415.
49)Kelsall, G. H., Welham, N. J., Diaz, M. A., 1993, “Thermodynamics of Cl-H_2O, Br-H2O, I-H2O, Au-Cl-H2O, Au-Br-H2O and Au-I-H2O Systems at 298 K”, Journal of Electroanalytical Chemistry, Vol. 361, pp. 13-24.

50) Atkins, P., de Paula, J., 2002, ”Physical Chemistry”, 7th Ed, W. H. Freeman and Company, New York, NY.

51) Pleysier, R., Dai, X., Wingate, C. J. and Jeffrey, M. I., 2008, “Microtomography Based Identification of Gold Adsorption Mechanisms, the Measurement of Activated Carbon Activity, and the Effect of Frothers on Gold Adsorption”, Minerals Engineering, Volume 21, Issue 6, pp. 453-462

52) Adams, M. D., 1995, “The Mechanism of Adsorption of Aurocyanide on to Activated Carbon, 1. Relation Between the Effects of Oxygen and Ionic Strength”, Hydrometallurgy, vol. 25, pp. 171-184.

53) Smith, J.M., 1986, “Chemical Engineering Kinetics”, McGraw-Hill Book Company, New Your, NY.

54) Karasyova, O N., Ivanova, L I., Lakshtanov, L Z., 1998, “Complexation of Gold(III)-Chloride at the Surface of Hematite”, Aquatic Geochemistry, Vol. 4, pp. 215-231.

55) Nechayev, Y., 1984, The effects of solution composition on the adsorption of gold(III) complexes on hematite. Geochem. Int., Vol. 21(4), pp. 87-93

56) Enzweiler, J., Joekes, I., 1991, “Adsorption of Colloidal Gold on Colloidal Iron Oxides”, Journal of Geochemical Exploration, Vol. 40. pp.133-142.

57) Ran, Y., Fu, J., Rate, A. W., Gilkes, R. J., 2001, “Adsorption of Au(I, III) Complexes on Fe, Mn Oxides and Humic Acid”, Chemical Geology, Vol. 185, pp. 33-49.

58) Mikhlin, Y. L., Romanchenko, A S., Asanov, I P., 2006, “Oxidation of Arsenopyrite and Deposition of Gold on the Oxidized Surfaces: A Scanning Probe Microscopy, Tunnelling Spectroscopy and XPS Study”, Geochimica et Cosmochimica Acta, Vol. 70, pp. 4874-4888.

59) Mycroft, J. R., Bancroft, G. M., McIntyre, N. S., Lorimier, J. W., 1995, “Spontaneous Deposition of Gold on Pyrite from Solutions Containing Au(III) and Au(I) Chloride. Part 1: A Surface Study”, Geochimica et Cosmochimica Acta, Vol. 59, No. 16, pp. 3351-3365.

60) Lagerge, S., Zajac, ., Partyka, S. and Groszek, A. J., 1999, “Comparative Study on the Adsorption of Cyanide Gold Complexes onto Different Carbonaceous Samples: Measurement of the Reversibility of the Process and Assessment of the Active Surface Inferred by Flow Microcalorimetry”, Langmuir, vol. 15, pp. 4803-4811.

61) Sun, T. M., Yen, W. T., 1993, ``Kinetics of Gold Chloride Adsorption Onto Activated Carbon``, Minerals Engineering, Vol. 6, No. 1, pp. 17-29.

62) Huges, H. C., Linge, H. G., 1989, “The Kinetics of Gold Loading from Gold(III) Chloride Solutions onto Fresh Activated coconut Carbon”, Hydrometallurgy, Vol. 22, pp. 57-65.

63) S. Baldwin, V.G. Papangelakis and G.P. Demopoulos, 1993, "Computer Simulation and Analysis of Pressure Oxidation Autoclaves Using REACTSIM", in Modelling, Simulation and Control of Hydromet. Processes, V.G. Papangelakis and G.P. Demopoulos (Eds.), CIM, Montreal, Quebec pp. 123-193.

64) S.A. Baldwin and G.P. Demopoulos, 1998, “Parameter Sensitivity of Kinetics-Based Hydrometallurgical Reactor Models”, Can. J. Chem. Eng., Vol. 76, pp. 1083-1092.

65) Pangum, L. S. And Browner, R. E.,1996, "Pressure Chloride Leaching of a Refractory Gold Ore", Minerals Engineering, Vol. 9, No. 5, pp. 547-556.

66) Milbourne, J., Tomlinson, M. and Gormely, L., 2003, "Use of Hydrometallurgy in Direct Processing of Base Metal/PGM Concentrates", Proceedings of Hydrometallurgy 2003- Fifth Conference in Honour of Professor Ian Ritchie- Volume 1: Leaching and Solution Purification, Young, C., alfantazi, A. Anderson, C., James, A., Dreseinger and Harris, B., TMS, Warrendale, PA, , pp. 617-630.

67) Ferron, C.J., Fleming, C. A., O'Kane, P. T. And Dreisinger, D., 2002, "Pilot Plant Demonstration of the Platsol Process for the Treatment of the NorthMet Copper-Nickel PGM Deposit", Mining Engineering, Vol. 54, No. 12, pp. 33-39.

68) Lakshmanan, V. I., Ramachandran, V. and Kondos, P. D., 2007 "Hydrometallurgy of Copper Concentrates: An Update", in Proceedings, The John E. Dutrizac International Symposium on Copper Hydrometallurgy, Vol IV, Book 1, pp. 101-128.

69) Defreyne, J., Grieve, W., Jones, D. L., Mayhew, K., 2006, The Role of Iron in the CESL Process. In Iron Control Technologies; Dutrizac, J. E., Riveros, P. A., Eds.; CIM, Montreal, QC, pp. 205-221.

70) Jennifer Defreyne, Tobias Cabral, 2009, "Early Copper Product Results from Vale's Hydrometallurgical CESL Refinery", paper presented at ALTA 2009 (accessed at www.cesl.com).

71) Hoffman, E. L., 1989, "Instrumental Neutron Activation Analysis as an Analytcal Technique for Gold Exploration", Journal of Geochemical Exploration, Vol. 32, pp. 301-308.

72) Brown, J. R., Deschenes, G., 1993, "Characterization of the Gold Complex Adsorbed on Activated Carbon from Chloride, Cyanide and Thiourea Solutions", CIM Bulletin, Vol. 85, No. 967, pp. 78-87.

73) Archibald, S. M., Migdisov, A. A., William-Jones, A. E., 2001, "The Stability of Au-Chloride Complex in Water Vapor at Elevated Temperature and Pressure", Geochimica et Cosmochimica Acta, Vol. 65, No. 23, pp. 4413-4423.

74) Bolorundo, S. A., Dreisinger, D. B. and Van Weert, G., 2003, "Fundamental Study of Silver Deportment During the Pressure Oxidation of Sulphide Ores and Concentrates", Miner. Eng., Vol. 16, pp. 695–708

APPENDIX A

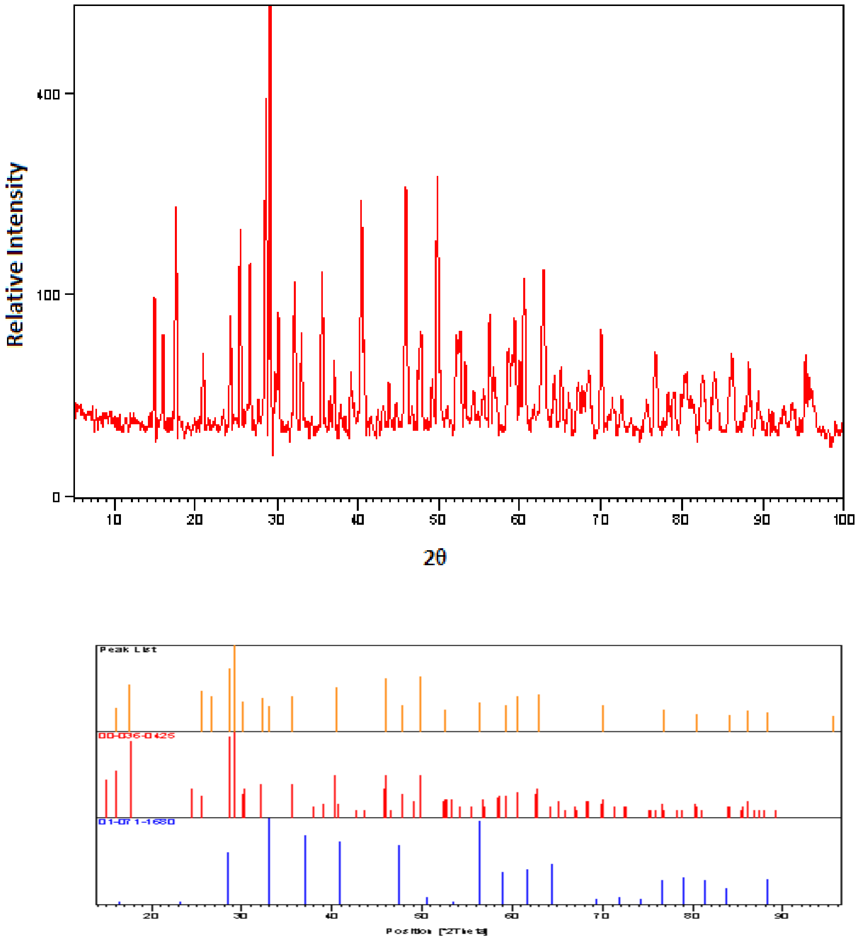

Figure A1: XRD of oxidation product of incomplete low pressure oxidation (30 min; pp. 64); below comparison of the residue XRD pattern with reference patterns (yellow = oxidation product, red = natrojarosite and blue = pyrite)

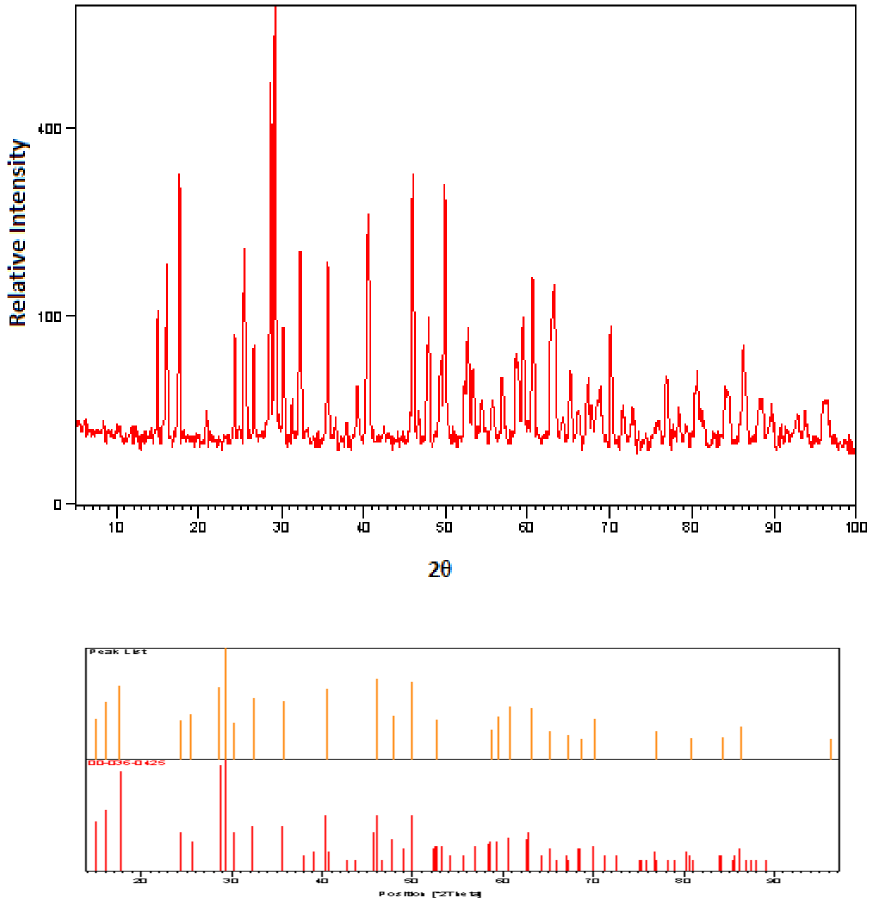

Figure A2: XRD of oxidation product of complete low pressure oxidation (4 hours pp. 64); below comparison of the residue XRD pattern with reference jarosite (yellow = oxidation product, red = natrojarosite)

Table 7: Atmospheric adsorption experiments: Extra data

TEMPERATURE	ACTIVATED CARBON	TIME (MIN)					
Low chloride (0.05M)		0	1	3	5	10	30
20 °C	20g/L	0.00%	74.33%	96.27%	100.00%	100.00%	100.00%
	15g/L	0.00%	63.70%	90.10%	99.92%	100.00%	100.00%
	10g/L	0.00%	60.00%	83.87%	93.87%	100.00%	100.00%
95 °C	20g/L	0.00%	76.33%	99.75%	100.00%	100.00%	100.00%
	15g/L	0.00%	73.80%	97.97%	99,85%	100.00%	100.00%
	10g/L	0.00%	61.33%	88.30%	99,73%	99,93%	100.00%
95 °C	20g/L	0.00%	82.00%	99.33%	100.00%	100.00%	100.00%
	15g/L	0.00%	72.50%	98.50%	100.00%	100.00%	100.00%
	10g/L	0.00%	71.00%	96.33%	99,67%	100.00%	100.00%
High chloride (1M)							
20 °C	20 g/L	0.00%	72.67%	90.23%	95.83%	98.33%	99.40%
95 °C	20 g/L	0.00%	76.33%	96.00%	99.03%	99.33%	99.63%